Particle Accelerators
1973, Vol. 5, pp. 129–154

PARTICLE ACCELERATION BY TEMPLATE MODIFIED COHERENT LIGHT

PAUL L. CSONKA†

Research Institute for Theoretical Physics, University of Helsinki, Helsinki 17, Finland
and
Institute of Theoretical Science‡ and Department of Physics, University of Oregon, Eugene, Oregon 97403, USA

A method is suggested to accelerate charged particles by intense bursts of monochromatic radiation of wavelength λ. Such radiation can be produced by lasers and is modified by a general optical element called 'template' which may be a holograph. Apart from the conventional optical elements all information is in the template, and when that is a holograph, it can be reproduced photographically. No magnets are needed. The ideal particle trajectory is straight and fully parallel to the electric field. Accelerating and focusing field elements have dimensions comparable to λ: high degree of miniaturization results. Assuming cylindrical geometry, a laser producing 10^{14} Watts instantaneous power, that the limit can be reached when the radial wavelength $\lambda_r \to \lambda$, the energy of a relativistic particle could be increased by about 180 GeV in 2 meters when the radiation coherence is maintained along the particle orbit. At such accelerations machine length can be reduced, vacuum and beam stability requirements can be relaxed, the beam cross section will tend to shrink, and damping due to synchrotion radiation may be significant. Heavy ions and unstable particles can be accelerated, positive and negative particles simultaneously. To reach higher energies, more than one laser are joined by 'synchronizers'.

1. INTRODUCTION

The present paper describes a method to accelerate particles with the help of intense coherent electromagnetic waves. Further calculational details can be found in Ref. 1.

Free electromagnetic radiation of momentum $\bar{k}$ exerts a force on charged particles through the well-known mechanism often referred to as radiation pressure. It was conjectured that this force may be responsible for accelerating at least some cosmic ray particles.[2] The average accelerating force is parallel to $\bar{k}$, and decreases as the particle momentum increases. This decrease can be avoided if the system is placed in a suitable longitudinal[3] or transverse[4] magnetic field, which induces a small transverse (to k) component $\bar{p}_\perp$ of the particle momentum $\bar{p}$, by causing the particle to spiral around $\bar{k}$, and then the acceleration along $\bar{k}$ is proportional to $p_\perp$.

The method of acceleration described in the present paper does not make use of any magnets, employs only optical elements and is well suited to accelerate relativistic particles. The ideal trajectory is straight. At any point along it, the electric field is fully parallel to the particle momentum $\bar{p}$, and the magnetic fields can be eliminated.

†Alfred P. Sloan Fellow
‡Permanent address

The properties of the proposed accelerator are summarized in Sec. 2. Accelerating configurations are described in detail in Sec. 3. The accelerating fields are produced by radiation from a laser modified by a general optical element called 'template', discussed in Sec. 4. The template can be a holograph. To reach higher energies, more than one laser is used. The lasers have to be synchronized to within a time interval π/ω, where ω is the angular frequency of the radiation. This can be achieved with the help of 'synchronizers' described in Sec. 5.

Equations are identified by two digits. The first digit refers to the section in which the equation occurs. The second gives the ordinal number of the equation within that section. In that section the equation is referred to by the second digit only, in all other sections by both digits. Thus Eq. (3.7) is the 7th equation in Sec. 3, is referred to as Eq. (7) within Sec. 3, and as Eq. (3.7) in all other sections.

2. GENERAL DESCRIPTION

In the proposed accelerator, acceleration of charged particles of charge q (hereafter simply referred to as 'particles') is accomplished by intense electromagnetic radiation.

For simplicity, we shall refer to the electromagnetic radiation as 'radiation'. Its wavelength, λ, is arbitrary.

The source of the radiation produces coherent radiation, but is otherwise arbitrary. Of particular interest is the case when the source is a laser. In the following, we shall refer to the source of coherent radiation simply as 'laser'; we do not intend to exclude thereby other sources of coherent electromagnetic radiation.

After leaving the laser, the radiation is directed to the trajectory of the particle to be accelerated, hereafter referred to simply as 'trajectory'.

On its way to the trajectory, the radiation is modified by a general optical element which controls the intensity, phase and polarization of the radiation. We shall refer to this general optical element as 'template'. The template determines the electric and magnetic field configuration at the trajectory. (See Fig. 1.) Except for certain restrictions imposed by technical limitations, any field configuration can be constructed in this manner, provided that it satisfies Maxwell's equations.

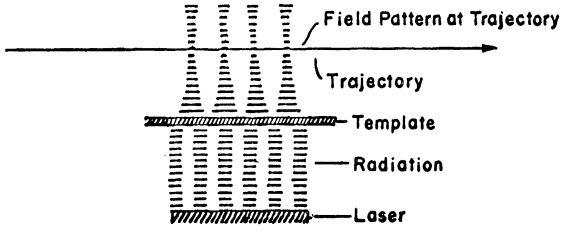

FIG. 1. The radiation travels from the laser to the trajectory. On its way it is modified by the template which produces the desired field pattern at the trajectory. Lenses, mirrors, etc., are not shown.

One laser (and the necessary lenses, mirrors, etc.) together with the template belonging to it can produce the desired accelerating field pattern. The laser (plus lenses, mirrors, etc.) and the template will be referred to as an 'accelerating unit'. Figure 1 shows one accelerating unit, the field produced by it, and the trajectory.

The radiation can be modified by the template either by transmission, or by reflection, or a combination of both. In practice, greater stability is to be expected if control is by reflection from a template surface. In the following, we will not distinguish between the various ways of control. We will simply say that the radiation passed 'through' the template, meaning that the radiation has passed that optical element, and the necessary information is now imprinted. We will indicate this schematically as in Fig. 1, even though in practice the radiation may not pass through the template, but be reflected from it.

The template can be prepared in several ways. First, one can calculate the values of the electric and magnetic field at the template, from their values at the trajectory and Maxwell's equations. This calculated information can then be inscribed on the template by irradiating it optically, or with other particles, e.g., ions. Second, one can use the techniques of holography[5] to produce a template which controls the intensity and to a large extent also the phase of the radiation passing through it. A conventional holograph does not control the phase completely, in addition to the desired image, it also permits the formation of the so-called 'twin-image'. The twin image can be eliminated, and later we shall make some remarks concerning it. When this is done, and the polarization is thus determined, we refer to the template as a 'phase controlled holograph'. In many cases complete phase control is not necessary, provided that radiation with the appropriate polarization is used. In such cases the template can be a conventional holograph.

Of interest are field configurations whose relevant spatial dimensions near the trajectory are comparable to λ. How to construct such field configurations is discussed in the later sections. One configuration is schematically shown in Fig. 2. In that figure, the trajectory is indicated by a dotted line. A cylindrically symmetric field pattern is constructed with the help of a cylindrical template, and with radiation which converges on the trajectory. One method is shown in Fig. 3. The radius R of the template cylinder is $\gg\lambda_r$, where λ_r is a typical 'radial wavelength' (of a cylindrical Bessel function). Due to this geometry, the fields are 'focused' along the trajectory, and are most intense within an imaginary cylinder (shown by dashed lines in Fig. 2) of diameter b, where b is of the order of λ_r. The field pattern consists of a succession of bright and dark areas. The length of these areas, d_b and d_d respectively, are comparable to λ. In the dark areas $\bar{E}$ and $\bar{B}$ are essentially zero. In Fig. 2, the electric and magnetic fields, $\bar{E}$ and $\bar{B}$ are shown at a particular moment. The $\bar{B}$ is circular, has zero value at the trajectory, increases

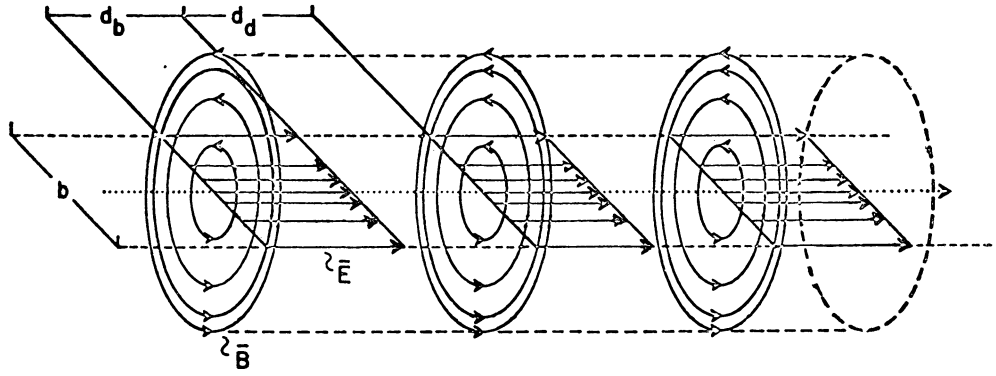

FIG. 2. Schematic picture of a field configuration discussed in Sec. 2. The trajectory is indicated by a dotted line. The electric and magnetic field lines, $\bar{E}$ and $\bar{B}$, are shown at one particular moment. The electric field lines are drawn in only one of those planes which contain the trajectory and are drawn only in the bright areas. For greater clarity, the magnetic field lines for each bright area are shown only in one plane perpendicular to the trajectory. The density of field lines drawn is roughly proportional to the corresponding field intensity. In fact, the fields in the dark areas are not exactly zero, div $\bar{E} = 0$ in vacuum, the transition between bright and dark areas is not as abrupt as in the figure, and is discussed in Sec. 3.

with distance roughly as a first order Bessel function, reaches a maximum, and then decreases. The electric field is highest at the trajectory and decreases away from it roughly as a zeroth order Bessel function. The exact transition between bright and dark areas will be discussed. The fields in the bright areas are not uniform, so the shown $\bar{E}$ and $\bar{B}$ really mean their average (over the z coordinate defined to be parallel trajectory) values.

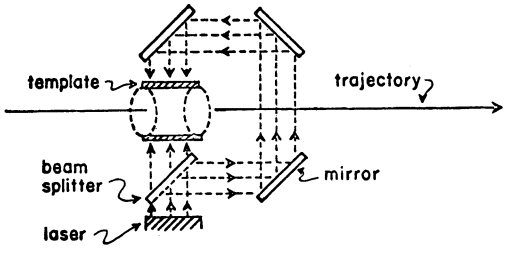

FIG. 3. Radiation produced by laser is divided by a beam splitter, and approaches the cylindrical template from opposite directions. The radiation can be divided more than once, and can be made to converge on the template from more than two directions.

Let us assume that we wish to accelerate positive particles. Similar considerations hold for negative particles. The particles are timed so that at the moment when they enter the first bright area, the $\bar{E}$ there is parallel to their velocity $\bar{v}$. They will experience a force parallel to $\bar{v}$, and be accelerated. After the particle leaves the first bright area, the $\bar{E}$ there decreases and eventually changes sign, but by the time (or shortly after) the electric force on the particle would reverse itself, the particle has already left the area, and is passing through the first dark region. The position of the bright areas is so chosen, that as the particle enters the next bright area, the electric field there again points parallel to $\bar{v}$, so that the particle is further accelerated, etc. Actually it is not necessary that the electric field be parallel to $\bar{v}$ all the time while the particle is in the bright area. All that is needed, is that the average field the particle experiences be parallel to $\bar{v}$.

Longitudinal focusing can be achieved by timing the particles so that they arrive at a bright spot at a moment when the electric field there is increasing in time. Particles which are delayed for some reason will then be accelerated more, while those which enter too soon will be accelerated less, or even decelerated. The electric field thus forms an 'electric bucket'.

Transverse focusing can be achieved by utilizing the magnetic field. This field oscillates in time. Half the time it has a direction as shown in Fig. 2, and the rest of the time it points in the opposite direction. During the time that its direction is as in Fig. 2, it will exert a restoring force on any positive particle which deviates from the ideal trajectory. For such particles, the magnetic field then forms a 'magnetic bucket'.

This magnetic field configuration focuses in *both* transverse directions, the horizontal one and the vertical one, simultaneously and with equal efficiency. It is thus a more effective focusing agent

than the standard quadrupole magnets. In general, no such efficient focusing can be achieved with static magnets, since for them curl $\bar{B} = 0$. By contrast, in our case curl $\bar{B} \neq 0$, precisely because we are working with non-static fields.

The electric and magnetic buckets do not necessarily overlap in time. However, for both positive and negative particles a time interval exists, when they do. This time interval is of the order of $T/8$, where T is the period of oscillation of the radiation. Particles which are timed to enter the field pattern during this time interval will be accelerated, and will be stable against both longitudinal and transverse momentum deviations. We will say that such particles are in an 'accelerating (electromagnetic) bucket'. Accelerating buckets for positive and negative particles do not occur at the same time and place, so both positive and negative particles can be simultaneously accelerated by the same field pattern. In addition, 'decelerating (electromagnetic) buckets' also exist, and these can be used to decelerate particles, should one wish to do so.

The accelerator consists of one or more accelerating units. If it consists of more than one, then two successive accelerating units are connected by elements which insure that particles will enter each unit at the right moment, and will be further accelerated by it (rather than decelerated, for example). These elements will be called 'synchronizers', and are discussed later in this paper.

If in each accelerating section an accelerated particle gains ΔK kinetic energy, then passing through a succession of N identical accelerating elements, its total energy gain will be

$$\Delta K_{\text{tot}} = N \Delta K. \tag{2.1}$$

Throughout most of the remaining part of this section, we list formulae which characterize the behaviour of the particle in the accelerator. Expressions for the wavelengths of longitudinal and transverse oscillations, momentum and energy acceptance, beam scattering on residual gases, beam self interactions, radiative, induction and absorption effects are given. Details of the straightforward but occasionally tedious calculations leading to these expressions can be found in Ref. 1 (where several of the relevant quantities are tabulated for various values of the parameters). The conditions under which these expressions are valid will be stated below.

The accelerating field is most efficient in accelerating particles along certain particular lines. We call such a line an 'ideal trajectory'. We consider field configurations in which only one ideal trajectory exists. Particles accelerated by accelerating buckets describe transverse and longitudinal oscillations in the vicinity of the ideal trajectory with wavelength $\lambda_\perp$ and $\lambda_\parallel$ respectively. In the following calculations, we assume that d_i, the characteristic dimensions along the trajectory of the accelerating field configuration satisfy

$$d_i \ll v \cdot \Delta t \tag{2.2}$$

$$v \cdot \Delta t \ll \lambda_\perp, \lambda_\parallel \tag{2.3}$$

where v is the particle velocity, and Δt is some suitable time interval.

For example, if the field is of the type shown in Fig. 2, then d_i can be either d_b or d_d, and both d_b and d_d have to satisfy Eqs. (2) and (3). In most cases of interest to us, a Δt satisfying Eqs. (2) and (3) can be found. We denote the average of the magnetic and electric fields experienced by the particle during the time interval $[t-(\Delta t/2), [t+(\Delta t/2)]$ by $\bar{B}_{\text{av}}(t)$ and $\bar{E}_{\text{av}}(t)$ respectively. The subscript 'av' will always mean averaging over Δt. We assume that the ideal trajectory is either straight, or its radius of curvature, R_c satisfies

$$R_c \gg \lambda_\perp, \lambda_\parallel. \tag{2.4}$$

We choose the z axis to be the tangent to the ideal trajectory. The radius vector measured from the z axis is $\bar{r}$, and the two components of $\bar{r}$ are x and y. The Cartesian axes x, y, and z form a right-handed system.

We denote the mass of the particle by m, its restmass by m_0, and

$$\gamma \equiv m/m_0, \tag{2.5}$$

$$\mathscr{E} \equiv mc^2. \tag{2.6}$$

The longitudinal (parallel to z) component is denoted by a subscript $\parallel$, e.g., $v_\parallel$. The transverse component is denoted by a subscript $\perp$, e.g., $\bar{v}_\perp$. The two Cartesian components of the transverse component are denoted by subscripts x and y, e.g., v_x, and v_y.

In cases of interest to us,

$$|v_\parallel| \gg |\bar{v}_\perp|, \tag{2.7}$$

and this will be assumed.

Everywhere in this paper, a quantity followed by a unit written in curly brackets means the value of the quantity immediately preceding the curly bracket measured in these units. For example, $\tau\{\text{sec}\}$ means the value of τ measured in seconds.

The force acting on the particle due to the accelerating field will be calculated according to the prescriptions of classical electrodynamical theory. At very high particle energies or field intensities corrections due to quantum effects may become significant, but will not be studied in this paper.

We assume that $\bar{F}$, that part of the force acting on the particle, which is due to the accelerating field configuration, satisfies

$$\begin{aligned} |F_{\perp \mathrm{av}}| = f_{\perp \mathrm{av}} \cdot r &= \frac{1}{r_M}\left|\left[\left(\frac{\bar{v}_{\|}}{c}\right)_M \times (\bar{B}_{\mathrm{av}}(t))_M \right.\right. \\ &\quad \left.\left. -(\bar{E}_{\perp \mathrm{av}}(t))_M\right] q \right| \cdot r \\ &\equiv \frac{1}{r_M}\left| q\left(\frac{\bar{v}_{\|}}{c}\right)_M (B_{\mathrm{av}}^{\mathrm{eff}}(t))_M \right| \cdot r; \text{ if } r < r_M \end{aligned} \tag{2.8a}$$

$$\Delta K = \Delta K_0\left(1 - \frac{z - z_0}{l/2}\right); \text{ if } |z - z_0| < l/2,$$

where $(B_{\mathrm{av}})_M$ and $(v_{\|}/c)_M$ are the maxima over one particle oscillation experienced by the particle of B_{av} and $v_{\|}/c$ respectively, $(B_{\mathrm{av}}^{\mathrm{eff}})_M$ is defined in Eq. (8a), ΔK is the energy gained by the particle while it passes through one accelerating bucket, z_0 is the z coordinate of the 'ideal particle', i.e., one which travels with a velocity v_0 such that when passing through the accelerator, it will acquire the most energy. The r_M and l are two constants characterizing the size of the accelerating bucket. For example, suppose that the accelerating field configuration is cylindrically symmetric around the ideal trajectory, and is of the type shown in Fig. 2. Consider the important special case when the electric field along the ideal trajectory varies as $e^{-i\omega t}(a_1 + a_2 \cos k_z z)$, where a_1 and a_2 are some constants. The discussion in Sec. 3 shows that in this case the magnetic and radial electric fields near the ideal trajectory vary as: constant $\cdot$, $e^{-i\omega t}(\cos k_z z)r$. Taylor expanding $F_{\|}$ and $F_{\perp}$ around z_0, $r = 0$, it can be seen that with the proper choice of z_0 and v_0 the conditions (2.8a) can be satisfied to a good approximation, so that the following expressions are valid to a good approximation for this field configuration.

In most cases of interest

$$\begin{aligned} [\partial(B_{\mathrm{av}}^{\mathrm{eff}})_M/\partial z]\lambda_{\perp} &\ll (B_{\mathrm{av}}^{\mathrm{eff}})_M \\ [\partial(\Delta K_0)/\partial z]\lambda_{\|} &\ll \Delta K_0 \end{aligned} \tag{2.8b}$$

Assuming this we find

$$\begin{aligned} \lambda_{\perp} &= 2\pi\left[\frac{\mathscr{E} r_M}{|q(B_{\mathrm{av}}^{\mathrm{eff}})_M|}\right]^{1/2}, \\ \lambda_{\|} &= 2\pi\gamma\left[\frac{mv_0 l}{2n\Delta K_0}\right]^{1/2}, \end{aligned} \tag{2.9}$$

where n is the number of accelerating buckets per unit length. The acceptance of the accelerator along any axis perpendicular to z, say the x axis (written as $A_x = \pi \cdot \text{length} \cdot \text{angle}$), is

$$A_x = \pi \frac{\pi}{\sqrt{2}} r_M\left[\frac{|q(B_{\mathrm{av}}^{\mathrm{eff}})_M|\, r_M}{\mathscr{E}}\right]^{1/2}, \tag{2.10}$$

and the energy acceptance

$$(\gamma - \gamma_0)_m = \gamma_0^{3/2}\left[\frac{l n \Delta K_0}{2 m_0 c^2}\right]^{1/2}, \tag{2.11}$$

where γ_0 is $(1 - v_0^2/c^2)^{-1/2}$. Even if $(\gamma - \gamma_0)$ exceeds the limit given by Eq. (11), the particle will be accelerated along the accelerator until it travels a distance

$$s \lesssim \frac{l}{2}\frac{(\gamma_0 \gamma)^{3/2}}{(\gamma - \gamma_0)_m}\left(\frac{v_0}{c}\right)^2 \tag{2.11a}$$

Some values of $\lambda_{\perp}$, $\lambda_{\|}$, A_x, $(\gamma - \gamma_0)_m/\gamma_0$, and s are listed in Table I.

Beam scattering on a residual gas in the channel causes a widening of the beam: the mean square of transverse beam oscillations, $\overline{r_m^2}$ increases in time. If the gas atoms have charge number Z_t, atomic number A_t, and their volume density is n_t, then due to Coulomb scattering.

$$\left.\frac{d\overline{r_m^2}}{dt}\right|_{\text{coul, gas}} = \frac{D_t}{-f_{\perp \mathrm{av}}}\frac{1}{v}\frac{1}{\gamma}, \tag{2.12a}$$

where

$$D_t \equiv (2.75 \cdot 10^{-21}\ \mathrm{cm}^2)\left(\frac{\mathrm{GeV}^2\, n_t G_t}{m_0}\right), \tag{2.12b}$$

TABLE I

A particle of charge q, rest energy $m_0 c^2$, and total energy $\mathscr{E}$ travels along a cylindrically symmetric accelerating channel whose effective radius is r_M. The $|q| = |e|$, where e is the electron charge. The particle oscillates in the transverse and longitudinal directions with wavelengths $\lambda_\perp$, and $\lambda_\parallel$. The acceptance along any axis perpendicular to the trajectory is A_x. The relative energy acceptance is $(\gamma-\gamma_0)_m/\gamma_0$ if the particle is to travel at least a distance s along the channel before being lost from the beam. The value $q(B_{\text{av}}^{\text{eff}})_M$ is assumed to be equal to $n\Delta K_0$, and both are assumed to be 1 GeV/cm for $r_M = 10^{-4}$ cm, and 3, 2 10^{-1} GeV/cm for $r_M = 10^{-3}$ cm. The t is assumed to be $r_M/4$.

$m_0 c^2$ in GeV	1				$5\cdot10^{-4}$			
$\mathscr{E}$ in GeV	10^2		10^6		10^2		10^6	
r_M in cm	10^{-4}	10^{-3}	10^{-4}	10^{-3}	10^{-4}	10^{-3}	10^{-4}	10^{-3}
$\lambda_\perp$ in cm	$6.3\cdot10^{-1}$	3.5	$6.3\cdot10$	$3.5\cdot10^2$	$6.3\cdot10^{-1}$	3.5	$6.3\cdot10$	$3.5\cdot10^2$
$\lambda_\parallel$ in cm	$1.6\cdot10$	$2.9\cdot10$	$1.6\cdot10^7$	$2.9\cdot10^7$	$3.6\cdot10^{-1}$	$6.5\cdot10^{-1}$	$3.6\cdot10^5$	$6.5\cdot10^5$
A_x in cm rad	$\pi\cdot2.2\cdot10^{-7}$	$\pi\cdot3.9\cdot10^{-6}$	$\pi\cdot2.2\cdot10^{-9}$	$\pi\cdot3.9\cdot10^{-8}$	$\pi\cdot2.2\cdot10^{-7}$	$\pi\cdot3.9\cdot10^{-6}$	$\pi\cdot2.2\cdot10^{-9}$	$\pi\cdot3.9\cdot10^{-8}$
$(\gamma-\gamma_0)_m/\gamma_0$ when $s=\infty$	$3.5\cdot10^{-2}$	$6.2\cdot10^{-2}$	$\gtrsim 1$	$\gtrsim 1$	$\gtrsim 1$	$\gtrsim 1$	$\gtrsim 1$	$\gtrsim 1$
s in cm when $(\gamma-\gamma_0)_m/\gamma_0 = 12\%$	1	1	10^8	10^8	1	1	10^8	10^8
s in cm when $(\gamma-\gamma_c)_m/\gamma_0 = 1.2\%$	10	10	10^9	10^9	10	10	10^9	10^9

$$G_t \equiv Z_t^2 \ln\left(\frac{3.84\cdot10^4}{(A_t Z_t)^{1/3}}\right). \tag{2.12c}$$

On the other hand, the fact that the beam is longitudinally accelerated, will cause the r_m to *shrink*.

$$\frac{d\overline{r_m^2}}{dt} = -\overline{r_m^2}\left(\frac{1}{\gamma}\frac{d\gamma}{dt} + \frac{1}{v}\frac{dv}{dt}\right). \tag{2.13}$$

If the beam is accelerated fast enough, then it may happen that the shrinking effect outweighs the spreading effect due to residual gas scattering, and the overall time derivative $d\overline{r_m^2}/dt$ is *negative*. This will happen in many cases of interest to us: the beam will shrink along its trajectory. The differential equation governing $\overline{r_m^2}$ can be obtained from Eqs. (12) and (13). Assuming that $d\gamma/dz$ is a constant in z, its solution is

$$\overline{r_m^2} = \left[\overline{r_m^2(\gamma_0)}\cdot\gamma_0 - \overline{r_l^2}\frac{\gamma^2-2}{\sqrt{\gamma^2-1}}\right]\frac{1}{\gamma} + \overline{r_l^2}\frac{\gamma^2-2}{\sqrt{\gamma^2-1}}\frac{1}{\gamma}. \tag{2.14}$$

As $\gamma \to \infty$,

$$\overline{r_m^2} \to \overline{r_l^2} \tag{2.15a}$$

where

$$\overline{r_l^2} \equiv \frac{D_t}{c^2\left|q(1/r_M)(B_{\text{av}}^{\text{eff}})_M\right|(d\gamma/dt)}, \tag{2.15b}$$

and in most cases of interest, the approach to $\overline{r_l^2}$ is essentially monotonic.

Strong interaction scattering will also have an effect on $\overline{r_m^2}(t)$. However, this effect is negligible compared to the terms on the right-hand side of Eq. (14). On the other hand, such scattering will cause a decrease in the volume density n_b of the beam particles

$$n_b(t) = n_b(t=0)\cdot e^{-t/\tau_s}, \tag{2.16a}$$

where in the limit $v \approx c$

$$\tau_s\{\text{sec}\} \approx \frac{1.1\cdot10^{15}}{n_t\{\text{cm}^{-3}\}A_t}, \tag{2.16b}$$

and the curly brackets indicate that in Eq. (16b) n_t is the value of n_t measured in cm^{-3} and then the equation gives τ_s in seconds. In most cases of interest to us τ_s is very long. Due to the decrease in n_b, energy is lost from the beam.

Coulomb scattering on the residual gas also causes energy loss from the strongly interacting particles, when $v \approx c$,

$$\frac{d\mathscr{E}/dt\big|_{\text{coul, gas}}}{d\mathscr{E}/dt\big|_{\text{strong, gas}}} \approx 2\cdot10^{-4}\frac{(\ln\gamma)Z_t^2}{\mathscr{E}\{\text{GeV}\}A_t}, \tag{2.17}$$

and is much smaller than unity for cases of interest to us. Therefore, to a good approximation, energy loss from the beam is due to strong interaction scattering.

Next we investigate how the particle trajectories are affected by the self interaction of the beam. We consider at first the case when the two beam particles interact electromagnetically with each other. These interactions we divide into two groups. First, cases when the relative velocity of the two particles is so high that the predominant interaction is low angle Coulomb scattering. Second, cases when the velocity is so low that collective static forces dominate. In both cases we evaluate only the dominant contributions.

Low angle beam-beam Coulomb scattering causes an increase in $\overline{r_m^2}$. Denoting by $w_\perp$ and $w_\parallel$ the average of the transverse and longitudinal speeds of the beam particles in the local beam rest frame, and provided that $w_\parallel \gg w_\perp$, one finds approximately

$$\left.\frac{d\overline{r_m^2}}{dt}\right|_{\text{coul, gas}} \approx \left.\frac{d\overline{r_m^2}}{dt}\right|_{\text{coul, gas}} \frac{n_b}{n_t}\frac{G_b}{G_t}\frac{1}{\gamma^2} \times \frac{cw_\perp}{w_\parallel^2}\ln\frac{w_\parallel}{w_\perp} \tag{2.18a}$$

where

$$G_b \equiv Z_b^2 \ln(\sqrt{\overline{r_m^2}}/r_b), \tag{2.18b}$$

and r_b is the effective radius of the beam particles. (When the beam particles are protons, r_b is the proton radius.) This equation is valid, provided that t is not too large. When t is very long, then $w_\perp$ has to be replaced by a different quantity, but in many cases of interest, Eq. (18) holds as it is written.

The presence of electric as well as magnetic static effects will modify $(B_M)_{\text{av}}$ and ΔK_0. Consequently, we have to correct Eqs. (7)–(12) and Eqs. (15), (17) and (18) by writing in them the modified values of $(B_M)_{\text{av}}$ and ΔK_0. This correction can be expected to become significant for these two quantities respectively, when the ratios

$$\left|\frac{f'_{\perp s}}{\gamma f_{\perp \text{av}}}\right| \equiv \frac{(4\pi/3)(R_\parallel/R_\perp)n_b q^2/\gamma}{\left|q(B_{\text{av}}^{\text{eff}})_M\right|/r_M} \tag{2.19a}$$

and

$$\left|\frac{f'_{\parallel s}}{\gamma f_{\parallel \text{av}}}\right| \equiv \frac{(4\pi/3)(R_\parallel/R_\perp)n_b q^2/\gamma}{2n\,\Delta K_0/\ell c^2\gamma^2} \tag{2.19b}$$

are larger than or of the order of unity. All symbols on the right-hand side of Eqs. (19) have been defined, except $R_\parallel/R_\perp$, which characterizes the beam, and is $\approx 1/4$ in many cases of interest to us.

The effect of static forces may be enhanced by instabilities, which greatly amplify random and originally small perturbations in the beam distribution. These effects are not completely understood. An approximate upper limit can be put on the magnitude of two of these effects, called the hose effect and sausage neck effect respectively. One finds that in cases of interest to us, these effects should become significant, if respectively

$$\frac{|(F_H)_m|}{|F_{\perp \text{av}}|} \equiv \frac{4r_M q^2}{\ell r_m}\rho_l \tag{2.20a}$$

(where ρ_l is the linear density of particles along the ideal beam),

and

$$\frac{|(F_{SN})_m|}{|F_{\parallel \text{av}}|} \equiv \left|\frac{qn_b r_m^2}{E_{\parallel \text{av}}}\right|. \tag{2.20b}$$

become comparable to or larger than unity.

Strong interaction beam-beam scattering will hardly change $\overline{r_m^2}$, but will decrease n_b. The decrease is proportional to n_b^2. For any given n_b, however, an 'instantaneous decay time', '$\tau_{s,\text{ beam}}$' can be defined, in analogy to τ_t. This quantity does depend on n_b, and, therefore, is put in quotation marks. One finds

$$\left.\frac{dn_b(t)}{dt}\right|_{\text{beam}} = \left.\frac{dn_b}{dt}\right|_{\text{gas}} \frac{n_b}{n_t}\frac{\Delta v}{v}\frac{A_b}{A_t}, \tag{2.21}$$

and

$$\text{'}\tau_{s,\text{ beam}}\text{'} \equiv \frac{1}{n_b \sigma_{s,b}\Delta v}, \tag{2.22}$$

where $\sigma_{s,b}$ is the strong interaction total cross section between beam particles, Δv is the average relative velocity of beam particles in the laboratory rest-frame and A_b is the atomic number of the beam particles. When we are dealing with a proton beam, the $A_b = 1$.

The oscillating particles emit synchrotron radiation, which in turn decreases the amplitude of oscillations. The radiation due to transverse oscillations dominates. The power radiated by these oscillations, averaged over one particle

oscillation, is[6]

$$P_{\perp \mathrm{Av}} = \frac{1}{3}\frac{q^4}{c^3 m_0{}^2}\gamma^2\left(\frac{1}{r_M}\overline{(B_{\mathrm{av}}^{\mathrm{eff}})_M}\right)^2 r_M{}^2\frac{v^2}{c^2} \quad (2.23)$$

As a result, the mean square amplitude decreases exponentially:

$$\overline{r_m{}^2(t)}_{\mathrm{Av}} = \overline{r_m{}^2(t=0)}_{\mathrm{Av}}\, e^{-t/\tau_r}, \quad (2.24a)$$

where

$$\tau_r \equiv \frac{3}{2}\frac{m_0{}^2c^4}{q^2c}\frac{1}{|q(B_{\mathrm{av}}^{\mathrm{eff}})_M/r_M|}\frac{1}{\gamma^2}. \quad (2.24b)$$

At the energies and fields which are of interest to us in this paper, the beam narrowing effect due to synchrotron radiation can be significant for not only electrons, but for protons as well. This effect can be utilized to further reduce the beam radius.[1]

While emitting a photon, the particles experience a recoil. This recoil is random, and will tend to increase $r_m{}^2$. An estimate of this effect yields

$$\overline{r_m{}^2(t)}_{\mathrm{Av}} \approx \frac{\overline{r_m{}^2(t=0)_{\mathrm{Av}}}}{1-t/\tau_R}, \quad (2.25a)$$

where

$$\tau_R \equiv \frac{3.2\cdot(m_0c^2)^4}{|q(B_{\mathrm{av}}^{\mathrm{eff}})_M/r_M|^2 q^2c^2\hbar\gamma}\frac{1}{\overline{r_m(t=0)_{\mathrm{Av}}}}. \quad (2.25b)$$

The two effects given in Eqs. (24) and (25) will cancel at the critical radius r_c, at which r_m will neither decrease or increase due to the emission of synchrotron radiation. We find

$$r_c = \frac{(m_0c^2)^2\gamma}{\hbar c\,|q(B_{\mathrm{av}}^{\mathrm{eff}})_M/r_M|}. \quad (2.26)$$

In cases of interest to us, τ_R is large, so that no significant increase in r_m will result over relevant time intervals.

As the radiation which produces the accelerating field passes through the beam, it will be attenuated. Assume cylindrical symmetry around the ideal trajectory, and slowly varying electric fields near the axis of symmetry. Denote by $|\bar{E}_{\|\mathrm{av}}^{\mathrm{v}}|$ the absolute value of $\bar{E}_{\|\mathrm{av}}$ when no beam is present. When the beam *is* present, then the electric field will differ from its vacuum value, and

$$|\bar{E}_{\|\mathrm{av}} - \bar{E}_{\|\mathrm{av}}^{\mathrm{v}}| \equiv \Delta E_{\|} \quad (2.27)$$

is no zero in general. Assume that $\Delta E_{\|}/|E_{\|\mathrm{av}}| \ll 1$. Then

$$|\bar{E}_{\|\mathrm{av}}(r)| \approx |\bar{E}_{\|\mathrm{av}}^{\mathrm{v}}| - 4\pi n_b |q|\frac{v}{c}r_M, \quad (2.28)$$

and is independent of r up to second order in $\Delta E_{\|}/|\bar{E}_{\|\mathrm{av}}^{\mathrm{v}}|$. When second order terms become significant, then this effect will tend to decrease as r decreases. Since the electric field in vacuum often decreases in second order with increasing r, with a proper choice of n_b this effect can be used to reduce the r dependence of the electric field in the beam below its vacuum dependence. The same effect can be used to increase the r dependence of the magnetic field.[1]

On the basis of these estimates and the formulae in Sec. 3, we can calculate the energy increase of a particle, which can be achieved with a laser capable of producing radiation bursts of $W = 10^{14}$ Watts instantaneous power, maintained over a few nanoseconds. In the theoretical limit, when $\lambda[1-(ck_z/\omega)^2]^{-1/2} \equiv \lambda_r \to \lambda$, and none of the radiation is lost due to unwanted reflections on optical elements before it had a chance to interact with the particle, when no twin image and no background term is produced by the templates, then a particle could be accelerated to about 270 GeV in 2 meters. In calculating this number we did assume that after one interaction with the particle the radiation is lost. In fact, with a sufficiently sophisticated template arrangement, the radiation would be utilized even after several reflections. This would further increase the energy gained by the particle for a given laser power. On the other hand, the background term and twin images produced by the templates are difficult to eliminate. Assuming that about half of the energy goes into construction of the background and twin images, the particle will gain about 190 GeV in 2 meters in the limit $\lambda_r \to \lambda$. However, this limit is difficult to approach technically, and detailed calculations will be needed to decide how close one can realistically hope to get to it. In the meanwhile, let us assume a relatively unsophisticated template structure. (See Table II.) Let us also assume that no specially designed injectors are available, but that we use one of the existing

TABLE II

The values of certain parameters are listed for a machine which contains two cylindrical templates: an 'inner' template with radius R_b and an 'outer' one with radius R_a. The $\langle F_\parallel \rangle$ is the average (over all z) force which accelerates the particle along the ideal trajectory, which is assumed to be straight and is chosen as the z axis. It is calculated from Eq. (3–15) with the assumption that the radiation power passing through the outer template is $5 \cdot 10^8$ watts/cm^2, that only 1/6 of total field energy is used efficiently for particle acceleration, and that the average of the force is $2^{-1/2}$ times its maximum value. The $\lambda_\perp$ is the wavelength (measured along z) of transverse (to z) particle oscillations, at injection into the accelerator calculated from Eq. (2–9). The A_x is the (horizontal or vertical) acceptance of machine (at injection) calculated from Eq. (2–10). All parameters are evaluated for several values of the total particle energy $\mathscr{E}$, and $\gamma \equiv \mathscr{E}/m_0 c^2$, where m_0 is the restmass of the particle. These values are chosen to be identical to the corresponding values for particles produced by the SLAC machine, a 300 GeV proton machine similar to the Batavia machine, and a fictitious 100 MeV electron machine with plausible parameters. These machines are assumed to inject into the accelerator particles which are then accelerated. All parameters are evaluated for two values of δ_b/λ, where $\delta_b \equiv \lambda_{zb} - \lambda$, the λ is the wavelength of the radiation in vacuum, and the accelerating field along the ideal trajectory is assumed to be of the form: const. $\{1 + \cos(2\pi z/\lambda_{zb})\}$. Even if λ_{zb} is appropriately chosen, only 1/6 of the total field energy is used efficiently for acceleration for fields of this form. When the value of δ_b/λ is not indicated in a certain row, then the quantities in that row are independent of δ_b/λ. The '(Number of accepted particles)/(Number of injected particles)' is obtained by dividing the (linear acceptance)^2 of the accelerator with the (linear emittance)^2 of the injector, and dividing this ratio by 8, because accelerating buckets are present only about one eighth of the time. If the number so obtained is $> 1/8$, then the correct value is 1/8. It is assumed that $|\Delta R_a|/\lambda = |\Delta R_b|/\lambda \equiv |\Delta R|/\lambda$, $|\Delta\lambda_{za}|/\lambda_{za} = |\Delta\lambda_{zb}|/\lambda_{zb} \equiv |\Delta\lambda_z|/\lambda_z$, $|\Delta L_a|/L_a = |\Delta L_b|/L_b \equiv |\Delta L|/L$, and to maximize $|\Delta\lambda|/\lambda$, choose $R_b = (\sqrt{2})R_a(\delta_b/\lambda)^{1/2}$. The tolerances are then calculated from Eqs. (3–39)–(3–42). The distance between mirrors inside the inner template is L_b, and outside the inner template it is $3.2 \cdot 10^2$ cm. The length of the accelerator is chosen to be 3.2 meters. It is assumed that both templates are appropriately coated, so that reflection losses are negligible. The inner template is a series of cylinders. Each of these cylinders, as well as the mirrors are located in low field regions of the radiation field. The dimensions of these regions (measured along z) are $\ll \lambda_\perp$, and are so chosen that these regions can be constructed with the help of propagating waves produced by the templates. It is assumed that the radiation is lost after 10 and 7 reflections on the inner side of the inner template when $\delta_b/\lambda = 5 \cdot 10^{-5}$ and $2.5 \cdot 10^4$ respectively. With more sophisticated template design it should be possible to make use of the radiation after even more reflections. The $D = 0.5$. The radiation is assumed to be produced by intense flashes of laser radiation, lasting for a few nseconds. The instantaneous radiation intensity is W, and for the stated parameters $W = 10^{14}$ watts $\cdot (R\{\text{in cm}\}10^{-2})$. The two quantities λ and R_a are left unspecified, and the dependence on them of the parameters is exhibited. The $\lambda\{\mu\}$ means the value of λ in microns. For example, if $\lambda = 3 \cdot 10^{-4}$ cm $= 3$ microns, $R_a = 100$ cm, so that $\lambda\{\mu\} = 3, (R_a/10^6\lambda) = 3.3 \cdot 10^{-1}$, then $W = 10^{14}$ watts; for $\delta_b/\lambda = 5 \cdot 10^{-5}$, and using SLAC as an injector, the $\langle F_\parallel \rangle = 3.0 \cdot 10^{-2}$ GeV/cm, $\lambda_\perp = 2.6 \cdot 10^2$ cm, about $1.3 \cdot 10^{-1}$ of all injected particles are accepted during the laser pulse, and the energy gain per particle during passage in the 3.2 meter long accelerator, is $\Delta\mathscr{E} = 9.6$ GeV. If $\lambda = 10^{-4}$ cm, $R_a = 100$ cm, so that $\lambda\{\mu\} = 1$, $(R_a/10^6\lambda) = 1$, then $W = 10^{14}$ watts; for $\delta_b/\lambda = 2.5 \cdot 10^{-4}$, when the SLAC machine is used as an injector, then the $\langle F_\parallel \rangle = 7.8 \cdot 10^{-2}$ GeV/cm, $\lambda_\perp = 44$ cm, about $5.6 \cdot 10^{-3}$ of the injected particles is accepted by the accelerator while the laser pulse lasts, and the accepted particles will increase their energy by $\Delta\mathscr{E} = 25$ GeV in 3.2 meters, etc.

		Machine used as injector		
	δ_b/λ	SLAC	100 MeV electron machine	300 GeV proton machine
γ		$4.0 \cdot 10^4$	$2.0 \cdot 10^2$	$3.0 \cdot 10^2$
$\mathscr{E}$ in GeV		$2.0 \cdot 10$	$1.0 \cdot 10^{-1}$	$3.0 \cdot 10^2$
$\left\|1 - \frac{\|\ \|}{c}\right\|$		$3.1 \cdot 10^{-10}$	$1.3 \cdot 10^{-5}$	$5.6 \cdot 10^{-6}$
Emittance in cm radian		$\pi \cdot 4 \cdot 10^{-6}$	$\pi \cdot 10^{-3}$	$\pi \cdot 5 \cdot 10^{-4}$
$\langle F_\parallel \rangle \cdot \left(\frac{R_a}{10^6\lambda}\right)^{-1/2}$ in GeV/cm	$5.0 \cdot 10^{-5}$ $2.5 \cdot 10^{-4}$	$5.2 \cdot 10^{-2}$ $7.8 \cdot 10^{-2}$	$5.2 \cdot 10^{-2}$ $7.8 \cdot 10^{-2}$	$5.2 \cdot 10^{-2}$ $7.8 \cdot 10^{-2}$
$\lambda_\perp \left(\frac{R_a}{10^6\lambda}\right)^{1/4} (\lambda\{\mu\})^{-1/2}$ in cm	$5.0 \cdot 10^{-5}$ $2.5 \cdot 10^{-4}$	$1.1 \cdot 10^2$ $4.4 \cdot 10$	8.0 3.1	$4.5 \cdot 10^2$ $1.8 \cdot 10^2$
$A_x \left(\frac{R_a}{10^6\lambda}\right)^{-1/4} (\lambda\{\mu\})^{-3/2}$ in cm.radian	$5.0 \cdot 10^{-5}$ $2.5 \cdot 10^{-4}$	$\pi \cdot 1.5 \cdot 10^{-6}$ $\pi \cdot 8.4 \cdot 10^{-7}$	$\pi \cdot 2.2 \cdot 10^{-5}$ $\pi \cdot 1.2 \cdot 10^{-5}$	$\pi \cdot 4.0 \cdot 10^{-7}$ $\pi \cdot 2.2 \cdot 10^{-7}$
$\frac{\text{(Number of accepted particles)}}{\text{(Number of injected particles)}} \cdot \left(\frac{R_a}{10^6\lambda}\right)^{-1/2} (\lambda\{\mu\})^{-3}, \lesssim 1/8$	$5.0 \cdot 10^{-5}$ $2.5 \cdot 10^{-4}$	$1.9 \cdot 10^{-2}$ $5.6 \cdot 10^{-3}$	$5.9 \cdot 10^{-5}$ $1.8 \cdot 10^{-5}$	$7.7 \cdot 10^{-8}$ $2.2 \cdot 10^{-8}$
$\frac{2L_b}{\lambda}$	$5.0 \cdot 10^{-5}$ $2.5 \cdot 10^{-4}$	$2.5 \cdot 10^3$ $5.0 \cdot 10^2$	$2.5 \cdot 10^3$ $5.0 \cdot 10^2$	$2.5 \cdot 10^3$ $5.0 \cdot 10^2$
$\|\Delta R\|/\lambda$		$1.3 \cdot 10^{-1}$	$1.3 \cdot 10^{-1}$	$1.3 \cdot 10^{-1}$
$\frac{\|\Delta\lambda\|}{\lambda}\left(\frac{R_a}{10^6\lambda}\right)$		$0.6 \cdot 10^{-7}$	$0.6 \cdot 10^{-7}$	$0.6 \cdot 10^{-7}$
$\frac{\|\Delta\lambda_z\|}{\lambda_z}\left(\frac{R_a}{10^6\lambda}\right) = \frac{\|\Delta L\|}{L}\left(\frac{R_a}{10^6\lambda}\right)$		$1.2 \cdot 10^{-7}$	$1.2 \cdot 10^{-7}$	$1.2 \cdot 10^{-7}$
$\Delta\mathscr{E}\left(\frac{R_a}{10^6\lambda}\right)^{-1/2}$ in GeV	$5.0 \cdot 10^{-5}$ $2.5 \cdot 10^{-4}$	$1.7 \cdot 10$ $2.5 \cdot 10$	$1.7 \cdot 10$ $2.5 \cdot 10$	$1.7 \cdot 10$ $2.5 \cdot 10$

machines (or machines similar to them) to inject particles into the accelerator. Table II shows that even under these relatively unfavourable conditions, quite high energy gains can be achieved. For example, when $W = 10^{14}$, $\lambda = 3 \cdot 10^{-4}$ cm and SLAC is used as an injector, with appropriate template choice one can achieve either that about a $1.3 \cdot 10^{-1}$ fraction of all injected particles are accepted and will gain 9.6 GeV in 3.2 meters, or that about a $5.6 \cdot 10^{-3}$ fraction of all injected particles are accepted and will gain 25 GeV in 3.2 meters.

So far (as in Table II), we assumed that after at most ten reflections the radiation is lost. Actually, the final design should be one in which the radiation is better utilized, and allowed to escape only after it transfers to the particles as much of its energy as possible. To achieve this, one would like to incorporate all templates inside the corresponding laser, at least when R_a is small. A laser lasing in a cylindrical mode seems particularly suitable for this purpose. The coherence properties of the radiation may thus also be improved. Ideally, the aim is to obtain an instrument from which very little radiation escapes, and most of the originally stored energy leaves in the form of fast particles. To what extent this may be achieved, can be decided only after a more detailed study.

In the accelerators described in this paper, there is no need for magnets, or metallic accelerating units. Most optical elements need not be made out of metal, and may be placed far from the beam. Detrimental charge and current induction effects on the beam may be further reduced by retardation effects, which can be significant for short pulses, because of the relatively large distances involved.

The high accelerating fields permit a reduction of the machine length: there is no need for long vacuum tunnels.

The acceleration time is correspondingly reduced: the particle can acquire a few hundred GeV within less than 10 nanoseconds, and up to 10^6 GeV within about 10 microseconds. Therefore, the beam has to remain stable only for such short times.

Due to extreme shortness of these times, the accelerators described here could accelerate not only the usual stable particles, but also shortlived unstable ones.

The large fields appear to make this method well suited for heavy ion acceleration. The fields can be so shaped that they will produce highly charged ions in the beam, and prevent effective recombination.

The large fields have the additional advantage that they accelerate the particles so fast, that the beam will not spread due to scattering on the residual gas, but will actually shrink continuously. They may induce synchrotron radiation intense enough to cause further beam shrinkage. Both effects contribute to beam stability.

The same field configuration can accelerate both positive and negative particle bunches either separately or simultaneously.

These types of accelerators will work well as the particle velocity $v \to c$, which is exactly the region of most interest to us.

Finally let us put the proposed method into perspective. Essentially, the method suggests a miniaturization of accelerators. The miniaturization is made possible by the short wavelengths λ, of intense coherent electromagnetic radiation which can be obtained today. The λ can be 10^{-4} cm or shorter. The accelerating and focusing field elements can now have dimensions comparable to λ. These elements correspond to accelerating cavities and focusing magnets, etc. in conventional accelerators. The dimensions of the conventional elements are several centimeters. The proposed miniaturization factor is, there about 10^{-4} or more. Due to the optical focusing properties of electromagnetic radiation, the fields in the miniaturized elements are correspondingly higher. These high fields open up a number of possibilities, as discussed above. Straightforward scaling down of conventional accelerators by a factor of 10^4 or more, and with a corresponding increase of field intensities is not technically possible: First, metal accelerating units with dimensions λ can not be manufactured, second, with such small scale units conventional methods of field generation can not be used, third, the correspondingly intense fields would destroy the accelerator. On the other hand, with the use of templates such miniaturization appears possible.

The fact that these high fields are produced by templates, has an additional advantage. There is no need to build magnets and other heavy equipment. Once a laser (plus mirrors, lenses, etc.) is

given, all additional information is contained in the template. If one wishes to change the parameters of the beam, the type, intensity, final energy or other parameter of the accelerator, one has only to change the template. Furthermore, some templates can be reproduced easily. When the template is a holograph, it can be reproduced by photographic means. In this case, if the necessary lasers (and lenses, mirrors, etc.) are available, and a new accelerator is needed, one does not have to build a new machine, it suffices to simply photograph an old one.

3. ACCELERATING FIELD CONFIGURATIONS

We denote the time coordinate by t, and the position vector in three space by $\bar{x}$. A hat, as in $\hat{z}$, denotes unit vector. The $\bar{x}$ will be specified either in terms of cartesian coordinates x, y, z, or in terms of cylindrical coordinates z, r and φ. The $\bar{z}$ is parallel to the axis of cylindrical symmetry, r measures the distance from it, and φ is an angle. We define

$$\hat{s} \equiv \hat{z} \times \hat{r}. \tag{3.1}$$

The vectors $\bar{A}(\bar{x})$, $\bar{E}(\bar{x})$ and $\bar{B}(\bar{x})$ will be specified either in terms of their components parallel to the x, y and z axes (e.g., $A_x(\bar{x})$, $A_y(\bar{x})$ and $A_z(\bar{x})$), or in the terms of their components parallel to the z, r, and s axes at the point $\bar{x}$: (e.g., $A_z(\bar{x})$, $A_r(\bar{x})$, $A_s(\bar{x})$).

We choose the electromagnetic vector potential in such a manner that in vacuum it satisfy

$$\Box \bar{A} = 0, \tag{3.2a}$$

$$\nabla \cdot \bar{A} = 0, \tag{3.2b}$$

and that the electric and magnetic fields be related to it by the equations

$$\bar{E} = -(1/c)\partial_t \bar{A}, \tag{3.3a}$$

$$\bar{B} = \bar{\nabla} \times \bar{A}. \tag{3.3b}$$

The most general $\bar{A}$ satisfying Eq. (2a) can be written as

$$A_i(t, \bar{x}) = \sum_{\omega_i', k_i', \nu_i'} c_{\omega_i', k_i', \nu_i'} e^{i(-\omega_i' t + k_i' z + \nu_i' \varphi)} J_{\nu_i'}(\kappa_i' r), \tag{3.4a}$$

where $i = x, y, z$,

$$\kappa_i' \equiv \left[\left(\frac{\omega_i'}{c}\right)^2 - k_i'^2\right]^{1/2}, \tag{3.4b}$$

and the c_i', k_i', ν_i', are arbitrary constants.

a) *Cylindrically Symmetric Fields*

Of special interest is the case, when

$$c_{\omega_i', k_i', \nu_i'} = \delta_{\omega_i', \omega} \cdot \delta_{\nu_i', 0} \cdot c_{k_i'}, \tag{3.5}$$

so that A_z oscillates harmonically as a function of time, and being independent of φ, is cylindrically symmetric. In this case, A_z can be written as

$$A_z(t, \bar{x}) = e^{-i\omega t} \sum_{kz} c_{k_z} e^{ik_z z} J_0(\kappa_z z). \tag{3.6a}$$

The following discussion is restricted to situations when the condition given by Eq. (6a) holds. Furthermore, we require that the field be periodic along z with a period $2L$. For such fields $n \equiv (\pi/L)k_z$ has to satisfy

$$n = \text{integer}. \tag{3.6b}$$

Finally, we impose the condition

$$A_s(t, \bar{x}) = 0. \tag{3.6c}$$

Substituting Eqs. (6) into Eq. (2b), we obtain

$$A_r(t, \bar{x}) = e^{-i\omega t} \sum_{k_z} c_{k_z} e^{ik_z z} \frac{(-ik_z)}{\kappa_z} J_1(\kappa_z r), \tag{3.7}$$

where $(\pi/L)k_z = \text{integer}$. It can be checked directly that $A_x = A_r \omega s\varphi$ and $A_y = A_r \sin \varphi$ satisfy Eq. (3.4), so that conditions (6) do not contradict Eqs. (2).

Having thus determined $\bar{A}(t, \bar{x})$ subject to the conditions (6), we evaluate the electric and magnetic fields. Substituting Eqs. (6) and (7) into Eqs. (3a) and (3b) one finds

$$E_z(t, \bar{x}) = \mathrm{Re}\left\{\frac{i\omega}{c} e^{-i\omega t} \sum_{k_z} c_{k_z} e^{ik_z z} J_0(\kappa_z r)\right\}, \tag{3.8a}$$

$$E_r(t, \bar{x}) = \mathrm{Re}\left\{\frac{i\omega}{c} e^{-i\omega t} \sum_{k_z} c_{k_z} e^{ik_z z} \frac{(-ik_z)}{\kappa_z} J_1(\kappa_z r),\right. \tag{3.8b}$$

$$E_s(t, \bar{x}) = B_z(t, \bar{x}) = B_r(t, \bar{x}) = 0, \tag{3.9}$$

$$B_s(t, \bar{x}) = \mathrm{Re}\left\{e^{-i\omega t} \sum_{k_z} c_{k_z} e^{ik_z z} \left(\frac{\omega}{c}\right)^2 J_1(\kappa_z r)\right\}. \tag{3.10}$$

Near the axis of cylindrical symmetry we can use the expansion

$$J_\nu(\kappa r) \underset{\kappa r \ll 1}{\approx} \sum_{l=0}^{N} \frac{(-1)^l}{l!\Gamma(\nu+l+1)}\left(\frac{\kappa r}{2}\right)^{2l+\nu}; \quad N < \infty \tag{3.11}$$

while for $\kappa r \to \infty$, we can approximate $J_\nu(\kappa r)$ by

$$J_\nu(\kappa r) \underset{\kappa r \to \infty}{\to} \left(\frac{2}{\kappa r \pi}\right)^{1/2} \cos\left(\kappa r - \frac{\pi}{4} - \nu\frac{\pi}{2}\right). \tag{3.12}$$

Substituting Eqs. (11) and (12) into Eqs. (8) and (10), we obtain

$$E_z(t,\bar{x}) \underset{\kappa_z r \to 0}{\to} \mathrm{Re}\left\{\frac{i\omega}{c} e^{-i\omega t}\sum_{k_z} c_{k_z} e^{ik_z z}\left[1 - \frac{(\kappa_z r)^2}{8} + \frac{(\kappa_z r)^4}{192} \pm \dots\right]\right\}, \tag{3.13a}$$

$$E_r(t,\bar{x}) \underset{\kappa_z r \to 0}{\to} \mathrm{Re}\left\{\frac{i\omega}{c} e^{-i\omega t}\sum_{k_z} c_{k_z} e^{ik_z z}(-ik_z)\left[\frac{r}{2} - \frac{\kappa_z^2}{32} r^3 + \frac{\kappa_z^4}{1152} r^5 \pm \dots\right]\right\}, \tag{3.13b}$$

$$B_s(t,\bar{x}) \underset{\kappa_z r \to 0}{\to} \mathrm{Re}\left\{e^{-i\omega t}\sum_{k_z} c_{k_z} e^{ik_z z}\left(\frac{\omega}{c}\right)^2\left[\frac{r}{2} - \frac{\kappa_z^2}{32} r^3 + \frac{\kappa_z^4}{1152} r^5 \pm \dots\right]\right\}, \tag{3.13c}$$

$$E_z(t,\bar{x}) \underset{\kappa_z r \to \infty}{\to} \mathrm{Re}\left\{\frac{i\omega}{c} e^{-i\omega t}\sum_{k_z} c_{k_z} e^{ik_z z}\left(\frac{2}{\pi\kappa_z r}\right)^{1/2} \cos\left(\kappa_z r - \frac{\pi}{4}\right)\right\}, \tag{3.14a}$$

$$E_r(t,\bar{x}) \underset{\kappa_z r \to \infty}{\to} \mathrm{Re}\left\{\frac{i\omega}{c} e^{-i\omega t}\sum_{k_z} c_{k_z} e^{ik_z z}\left(\frac{2}{\pi\kappa_z r}\right)^{1/2}\left(\frac{-ik_z}{\kappa_z}\right)\sin\left(\kappa_z r - \frac{\pi}{4}\right)\right\}, \tag{3.14b}$$

$$B_s(t,\bar{x}) \underset{\kappa_z r \to \infty}{\to} \mathrm{Re}\left\{e^{-i\omega t}\sum_{k_z} c_{k_z} e^{ik_z z}\frac{(\omega/c)^2}{\kappa_z}\left(\frac{2}{\pi\kappa_z r}\right)^{1/2} \sin\left(\kappa_z r - \frac{\pi}{4}\right)\right\}. \tag{3.14c}$$

Equations (13a) and (14a) show that the amplitude of the electric field near the axis exceeds that of the electric field at some large distance R from the axis by the factor

$$\frac{|E_z(r=0)_{\max}|}{|E_z(r=R)_{\max}|} = \pi\left(\frac{R}{\lambda_r}\right)^{1/2}, \tag{3.15}$$

and a similar equation holds for the magnetic field. The amplification of the fields near the axis is, of course, due to the focusing property of the cylindrical geometry, and can be quite large. The E_z and B_s do not reach their maximum value at the same moment, there is a shift of a quarter period: $\pi/2\omega$, between them. The maxima nearest to the axis of B_s occur at a distance $\approx(\lambda_r/4)$ from the axis of symmetry. The λ_r can be called the 'radial wavelength', is defined as

$$\lambda_r \equiv \lambda\left[1 - \left(\frac{ck_z}{\omega}\right)^2\right]^{-1/2}, \tag{3.16}$$

and $\lambda_r \to \lambda = (c\omega/2\pi)$ as $k_z \to 0$.

The appropriate boundary conditions at $z = \pm L$ would be insured if the cylinder could be closed by two perfect mirrors located at $z = \pm L$, both perpendicular to z, provided that the field configuration is appropriately chosen. With realistic mirrors some deviation from the desired boundary conditions is unavoidable. Openings can be made in the mirrors near the axis to permit the particles to enter and leave the accelerating field configuration. These openings will cause further deviation from the desired boundary conditions.

To avoid excessive energy transfer to the mirrors, they can be located at z values at which both the electromagnetic energy flux is small. The mirrors can be located in a long template cylinder wherever the phase difference between the particle and the accelerating field reaches $(2m+1)\pi$, (m : integer), so that after passing the mirror, the particle again finds itself in phase with the accelerating field. If at $z = 0$ the particle is in phase with the field, then the smallest $2L$ for which the phase is π, is $L = (\lambda/\omega)\pi v_0[\lambda - (2\pi v_0/\omega)]^{-1}$.

b) *The Coefficients* c_{k_z}

The coefficients c_{k_z} are so far arbitrary. We will specify them in such a manner that they insure the greatest possible energy transfer to a particle which travels along the z axis.

Let us assume that the field configuration under discussion is produced by monochromatic radiation, with frequency ω and wavelength λ, which passes through a cylindrical template and converges on the axis. The radius of the template cylinder is R, the cylinder extends from $z = -L$ to $z = +L$, so that it is $2L$ long. The energy density of the radiation within the cylinder is

$$U = \frac{1}{8\pi}(\bar{E}^2 + \bar{B}^2). \tag{3.17}$$

Averaged over the period of the radiation: $T \equiv 2\pi/\omega$, the total radiation energy in the cylinder is

$$\varepsilon = \frac{\omega}{2\pi}\int_0^{2\pi/\omega} dt \int_{-L}^{+L} dz \int_0^R dr\, r 2\pi U. \tag{3.18}$$

We are mainly interested in the case when $R\kappa_z \gg 1$ for most κ_z occurring in Eqs. (8) and (10). Then Eqs. (14) are a good approximation over most of the cylinder volume. We substitute Eqs. (14) into Eq. (17), and that, in turn, into Eq. (18) and obtain

$$\varepsilon \approx \frac{2LR}{2\pi}\sum_{k_z} |c_{k_z}|^2 \left(\frac{\omega}{c}\right)^2 \kappa_z^{-3}. \tag{3.19}$$

This expression is valid, provided that $\kappa_z \gg 1/R$ for most κ_z values occurring in the sum.

Next we calculate ΔK, the kinetic energy gained by a particle of charge q, after entering the cylinder at $t = 0$ at $z = -L$, as it travels along the axis from $z = -L$ to $z = +L$ with a velocity $v(z)$ which may be a function of z. We denote by $u(t)$ the average velocity between $t = 0$ and $t = t'$, defined as

$$u(z') = \frac{z(t')}{t'}, \tag{3.20}$$

where $z(t')$ is the position of the particle at t' along the axis. Making use of Eq. (13a), ΔK can be expressed as

$$\Delta K(L, -L) = q\int_{-L}^{L} dz\, E_{\|}(z)$$

$$= \mathrm{Re}\left\{ iq\frac{\omega}{c}\sum_{k_z} c_{k_z} \int_{-L}^{+L} dz\, e^{i[k_z - (\omega/u(z))]z}\right\}. \tag{3.21}$$

We are particularly interested in the case when the velocity $v(z)$ changes slowly as a function of z. Such is the case when $E_{\|}$ is small, and, which is more relevant, when $v \approx c$. In this case

$$v(z) = v_0 + \frac{a_0}{v_0} z + \ldots \approx v_0 + \frac{a_0}{v_0} z \tag{3.22}$$

and

$$\Delta K(L, -L) \approx \mathrm{Re}\left\{ iq\frac{\omega}{c}\sum_{k_z} c_{k_z} \frac{e^{-i\beta^2}}{\alpha} \times \sqrt{\frac{\pi}{2}}[C(w) + iS(w)]_{w=\sqrt{(2/\pi)}(-\alpha L+\beta)}^{\sqrt{(2/\pi)}(\alpha L+\beta)}\right\} \tag{3.23}$$

where

$$\alpha \equiv \left[\frac{\omega a_0}{v_0 3}\right]^{1/2}$$

$$\beta \equiv \frac{1}{2\alpha}\left(k_z - \frac{\omega}{v_0}\right)$$

and the $C(x)$ and $S(x)$ are the well known Fresnel integrals. If

$$\frac{a_0}{v_0} z \ll 1 \tag{3.24}$$

then, over short enough intervals in z, we can write $\alpha \approx 0$, $v \approx v_0$. With this approximation Eq. (21) gives

$$\Delta K(L, -L) \approx \sum_{k_z} \mathrm{Re}\left\{ c_{k_z} 2iq\frac{\omega}{c}\frac{\sin\,(k_z - (\omega/v_0))L}{k_2 - (\omega/v_0)}\right\}. \tag{3.25}$$

Since in the Fourier sum the k_z can assume only those values for which $k_z L/\pi = \text{integer}$, one can always rewrite $\sin[k_z - (\omega/v_0)]L$ as $(-1)^{(k_z L/\pi)+1} \cdot \sin(\omega L/v_0)$.

The accelerating field configuration is to be produced with the help of a cylindrical template as described before Eq. (17). This fact puts some restrictions on the values of k_z which can contribute to E and B through Eqs. (8) and (10). In fact, since the radiation frequency is ω, waves with $|k_z| > \omega/c$ will not propagate inside the cylinder, but will be

completely reflected from its surface. We are mostly interested in the case when $R \gg \lambda_r$. Then the completely reflected waves will not contribute significantly along the cylinder axis, and for all practical purposes, the contribution of all waves with $|k_z| > \omega/c$ can be neglected. Hereafter, whenever $R \gg \lambda_r$, summation over k_z is understood to be taken from $-(\omega/c)$ to $+(\omega/c)$.

We intend to choose the field configuration in such a manner that $\Delta K(L, -L)$ be maximum for any given value of ε. This requirement will determine those c_{k_z} for which $|k_z| \leqq \omega/c$, according to the equation

$$0 = \frac{\partial}{\partial c_{k_z}}[\Delta K(L, -L) - \Lambda\varepsilon], \tag{3.26}$$

where Λ is a Lagrange multiplier. Substituting Eqs. (19) and (25) into Eq. (26), one finds

$$c_{k_z} = \frac{i\pi q}{\Lambda^* RL}\frac{c}{\omega}\left[1-\left(\frac{ck_z}{\omega}\right)^2\right]^{3/2} \times \frac{(-1)^{k_z L/\pi}\sin[(\omega/v_0)L]}{[(ck_z/\omega)-(c/v_0)]}. \tag{3.27}$$

With this choice of c_{k_z}, the ΔK will assume its maximum value of

$$\Delta K(L, -L) \approx \sum_{k_z=-\omega/c}^{\omega/c} \mathrm{Re}\left\{\frac{1}{\Lambda^*}\right\}\frac{2\pi q^2}{RL}\frac{c}{\omega} \times\left[1-\left(\frac{ck_z}{\omega}\right)^2\right]^{3/2}\frac{\sin^2[(\omega/v_0)L]}{[(ck_z/\omega)-(c/v_0)]^2}. \tag{3.28}$$

This expression is valid, if for most k_z occurring in the sum, $\kappa_z \gg 1/R$. The Λ is a multiplicative normalization constant, which can be expressed in terms of ε by substituting Eq. (28) into Eq. (19). However, for our purposes the value of Λ will turn out to be irrelevant, so we leave it in Eq. (28).

In most cases of interest, it is easy to change the length of the template by an amount ΔL which is comparable to $Tv_0 = (2\pi v_0/\omega)$. Choosing

$$L = (\tfrac{1}{2}+m)\frac{\pi v_0}{\omega};\ m\text{: integer}, \tag{3.29}$$

the absolute value of c_{k_z} and ΔK reach a maximum in the neighborhood of any $L > Tv_0$.

Equations (25), (27), (28) and (29) have simple interpretations in terms of the energy transferable to a charged particle by an electromagnetic plane wave. This is discussed in Appendix 1. Accordingly, one expects that for efficient energy transfer from a Fourier component, one has to have $\Omega_z L \equiv 2\pi[(1/\lambda_z)-(\omega/2\pi v_0)]L \approx \pi/2$. This is discussed in Appendix 1.

From Eqs. (19) and (28) it is obvious that simply focusing the light on a small spot along the trajectory would be a very *inefficient* way of trying to accelerate a particle. Indeed, focusing the light on a spot of diameter of the order of λ, produces a field configuration which is a 'delta function of width λ', i.e., a function such that c_{k_z} is approximately a constant for all λ_z between λ and $2L$, and is zero for all other λ_z. The number of nonzero c_{k_z} is of the order of $2L/\lambda \equiv N$. According to Eq. (19), the energy stored in each of these Fourier components (except when $\lambda_z \approx \lambda$) is of the same order of magnitude: ε/N. Only that component will accelerate efficiently for which $\Omega_z L \approx \pi/2$. The amplitude of this component is of the order of $\sqrt{\varepsilon/N}$, so that approximately $\Delta K \sim N^{-1/2}$. Since $N \sim L$ and $N = 1$ for $2L = \lambda$, the efficiency of such device compared to the one described by Eq. (27) is approximately $\sqrt{\lambda/2L}$, usually a very small number. The same result can be understood by imagining that radiation is focused on a strip of length (along the trajectory) $2L$, and width λ. If the total energy of the field, and λ are both fixed, then the density of the field energy is proportional to $(2L)^{-1}$: $U \sim (2L)^{-1}$. The amplitude of the electric field $E_0 \sim U^{1/2} \sim (2L)^{-1/2}$, and the kinetic energy acquired by the particle along the strip $\Delta K \sim E_0 2L \sim (2L)^{1/2}$. The factor gained in ΔK is, therefore, approximately $\sqrt{\lambda/2L}$. In the last argument we assumed that the field accelerates continuously along the strip. This is not true for $2L > \lambda$, but the average over a length comparable to λ_z, can be continuous, e.g., in the case of the field configuration described in Eq. (27). We conclude that instead of focusing the radiation, one should 'spread it out' along the trajectory.

Equations (27) and (28) were derived under the assumption that the velocity is approximately a constant. They give good approximations to the values of c_{k_z} and ΔK as long as

$$2L \gg \frac{{v_0}^2}{a_0}. \tag{3.30}$$

If this condition is not fulfilled, then Eqs. (27) and (28) can still be used by dividing up the cylinder into sections of length $2L_j$, where Eq. (29) is satisfied within each section, and provided that for each section one has $2L_j \gg \lambda$. If the velocity changes significantly along the cylinder axis within a distance comparable to λ, then Eq. (23) can be used, provided that the change in acceleration is not too fast. In the contrary case, expression (21) is to be worked out for the particular $v(z)$ function in question.

c) *Tolerances*

Next we estimate the tolerances within which the parameters of the accelerator may deviate from their ideal value. The following estimates refer to a cylindrical template, in which radiation with angular frequency $\omega = 2\pi c/\lambda$ generates an accelerating field configuration with one given value of λ_z. At first we consider the parameters R, L, λ and λ_z, their deviation from their ideal values will be denoted by ΔR, ΔL, $\Delta\lambda$ and $\Delta\lambda_z$ respectively.

Assume that near the trajectory (i.e., when $r \lesssim \frac{1}{4}\lambda_r$), the relative error of the average (over $\lambda_\perp$) of the absolute value of the electric field[6], $\Delta|\bar{E}|_{\mathrm{Av}}/|\bar{E}|_{\mathrm{Av}}$, and that of the magnetic field, $\Delta|\bar{B}|_{\mathrm{Av}}/|\bar{B}|_{\mathrm{Av}}$, are required to satisfy

$$\begin{aligned} D_E &\equiv \Delta|\bar{E}|_{\mathrm{Av}}/|\bar{E}|_{\mathrm{Av}} \lesssim D, \\ D_B &\equiv \Delta|\bar{B}|_{\mathrm{Av}}/|\bar{B}|_{\mathrm{Av}} \lesssim D, \\ D &\ll 1. \end{aligned} \tag{3.31}$$

If $\Delta R \neq 0$, and $\Delta L = \Delta\lambda = \Delta\lambda_z = 0$, then D_E and D_B at some point near the trajectory is $\lesssim 4\Delta R/\lambda_r$, whenever $\Delta R/\lambda_r \ll 1$. Therefore, to satisfy requirements (31), one needs

$$|\Delta R| \lesssim D\frac{\lambda_r}{4} = \frac{D}{4}\lambda\left[1-\left(\frac{\lambda}{\lambda_z}\right)^2\right]^{-1/2}. \tag{3.32}$$

If $\Delta\lambda \neq 0$, and $\Delta R = \Delta L = \Delta\lambda_z = 0$, then the deviation $\Delta\lambda_r$ of λ_r from its ideal value will satisfy $|\Delta\lambda_r| \approx \lambda_r$. $(|\Delta\lambda|/\lambda)[\lambda_z^2/(\lambda_z^2-\lambda^2)]$ as $|\Delta\lambda_r| \to 0$. The D_E and D_B are $\approx [4(\Delta\lambda_r)R/\lambda_r^2]$. Therefore, requirements (31) imply

$$\frac{|\Delta\lambda|}{\lambda} \lesssim \frac{D}{4}\frac{(\lambda_z^2-\lambda^2)^{1/2}}{\lambda_z}\frac{\lambda}{R}. \tag{3.33}$$

If $\Delta\lambda_z \neq 0$, $\Delta L = (\Delta\lambda_z)L/\lambda_z$, and $\Delta R = \Delta\lambda = 0$, then $|\Delta\lambda_r|/\lambda_r \approx (|\Delta\lambda_z|/\lambda_z)([\lambda^2/(\lambda_z^2-\lambda^2)]$ whenever $|\Delta\lambda_r| \to 0$. By the same arguments which lead to Eq. (33), we find that requirements (31) can be satisfied only if

$$\frac{|\Delta\lambda_z|}{\lambda_z} \lesssim \frac{D}{4}\frac{(\lambda_z^2-\lambda^2)^{1/2}}{\lambda}\frac{\lambda_z}{R}. \tag{3.34}$$

If $\Delta L \neq 0$, $\Delta R = \Delta\lambda = \Delta\lambda_z = 0$, and z_c is the position of points along the trajectory where the electric field has a certain phase at a given moment, then $|\Delta z_c| \approx (R/L)|\Delta L|(\lambda/\lambda_z)[1-(\lambda/\lambda_z)^2]^{-1/2}$ for $\Delta L \to 0$. When $|\Delta z_c|/\lambda_z \ll 1$, the D_E and D_B are $\approx 4|z_c|/\lambda_z$, and to satisfy conditions (31) one has to have

$$\frac{|\Delta L|}{L} \lesssim \frac{D}{4}\frac{\lambda_z}{\lambda}\frac{(\lambda_z^2-\lambda^2)^{1/2}}{R}. \tag{3.35}$$

The mirror surface should be smooth approximately within an accuracy of $|\Delta L|$ given in Eq. (35).

Systematic errors in the template pattern $f(z)$ (where f can be the reflexitivity, absorbitivity, or optical thickness) will cause a $\Delta\lambda_z$ to appear. The tolerances on this are given by Eq. (34). Random errors will cause the appearance of unwanted Fourier components. The net acceleration or deceleration of the particle due to these will be negligible, but their presence is wasteful, because the radiation energy, ΔU, stored in them is not used efficiently for acceleration. From Eq. (19)

$$\begin{aligned} \frac{\Delta U}{U} &\approx \sum_{\substack{\text{unwanted}\\ k_z}} |c_{k_z}|^2 \frac{\left(\frac{\omega}{c}\right)^2}{\kappa_z^3} \Bigg/ \sum_{\substack{\text{wanted}\\ k_z}} |c_{k_z}|^2 \frac{\left(\frac{\omega}{c}\right)^2}{\kappa_z^3} \\ &\approx \frac{\int_{-L}^{L} dz\,|\Delta f(z)|^2}{\int_{-L}^{L} dz\,|f(z)|^2}. \end{aligned} \tag{3.36}$$

Let us assume that the mirror material can tolerate a field which is α_m times the average value of the absolute value of the field prevailing at r values in the range $(r_m + \lambda_r)$, where r_m is the r coordinate of that mirror point which is closest to the axis. Then one has to have

$$\frac{|\Delta f|_{\mathrm{Av}}}{|f|_{\mathrm{Av}}} \lesssim \alpha_m \begin{cases} \left(\frac{L}{3\lambda}\right)^{1/2}; & \text{at points where errors in Fourier components add randomly} \quad (3.37a) \\ 1; & \text{at points where they all add coherently} \quad (3.37b) \end{cases}$$

$D \lesssim \alpha_m$.

The dark areas near the mirrors can be extended by choosing c_{k_z} appropriately, e.g., let the k_z occur in pairs so that whenever a k_z occurs, either $c_{k_z} \approx -c_{k_{z+1}}$ or $c_{k_z} \approx -c_{k_{z-1}}$. To insure that during turning on (and off) of the radiation the deviation from the ideal field configuration will not damage the mirrors (and possible other optical elements to be discussed below), the field intensity can be allowed to increase (and decrease) linearly during a time interval τ. The τ can be chosen to be larger or equal to any one of the τ_i. Here the τ_i is the time interval which is needed for switching on (or off) of the field, if the field changes linearly in time and an optical element located at a point $\bar{x}_i$, can tolerate a field which is α_i times the average of the absolute value of the field prevailing at r values in the range $(r_i + \lambda_r)$. If the optical element is located in a relatively low field region of the standing wave pattern when the field is considered as a function of r near $\bar{x}_i$ then

$$\tau_i \gtrsim \frac{1}{\alpha_i}\frac{2r_i}{c}\left[1-\left(\frac{\lambda}{\lambda_z}\right)^2\right]^{-1/2}, \qquad (3.38a)$$

because such a region is the result of the interference of cylindrical waves approaching $\bar{x}_i$ from opposite radial directions. If the optical element is located in a relatively low field region when the field is considered as a function of z near $\bar{x}_i$, then

$$\tau_i \gtrsim \frac{1}{\alpha_i}\frac{1}{c}\sqrt{(R-r)^2+L'^2} \lesssim \frac{1}{\alpha_i c}[R^2+L^2/4]^{1/2} \qquad (3.38b)$$

because the low field region is a result of interference of waves originating at points of the template which are located at a distance not more than L' from each other, where $L' \leqq L/2$.

So far we considered the simplest case: that of one template. The requirements on the tolerances can be reduced by employing two or more templates, placed within each other. As an example, consider two cylindrical templates, with radii R_a and R_b respectively, $R_a > R_b$. The inner template creates the 'inner' field which accelerates the particles. The outer template focusses the radiation on the inner one, and sets up the 'outer' field pattern. The outer field pattern has a minimum at the inner template, so that the latter is located at an essentially electric field free region. The mirrors in the inner and outer fields are located at distances L_a and L_b from each other, at low flux regions of the outer and inner fields respectively. Consider the situation when the relevant wave lengths in the outer and inner fields are λ_{za} and λ_{zb} respectively. The tolerances can be calculated similarly to the case when only one template exists. In particular, we now have instead of Eqs. (32)–(35):

$$D \gtrsim 4\frac{|\Delta R_a|}{\lambda}\left[1-\left(\frac{\lambda}{\lambda_{za}}\right)^2\right]^{1/2} + 4\frac{|\Delta R_b|}{\lambda} \times \left[1-\left(\frac{\lambda}{\lambda_{zb}}\right)^2\right]^{1/2}, \qquad (3.39)$$

$$D \gtrsim 4\frac{|\Delta\lambda|}{\lambda}\left\{\frac{R_a}{\lambda}\lambda_{za}(\lambda_{za}^2-\lambda^2)^{-1/2} + \frac{R_b}{\lambda}\lambda_{zb}(\lambda_{zb}^2-\lambda^2)^{-1/2}\right\}, \qquad (3.40)$$

$$D \gtrsim 4\frac{|\Delta\lambda_{za}|}{\lambda_{za}}\frac{R_a\lambda}{\lambda_{za}}(\lambda_{za}^2-\lambda^2)^{-1/2} + 4\frac{|\Delta\lambda_{zb}|}{\lambda_{zb}}\frac{R_b\lambda}{\lambda_{zb}}(\lambda_{zb}^2-\lambda^2)^{-1/2} \qquad (3.41)$$

$$D \gtrsim 4\frac{|\Delta L_a|}{L_a}\frac{R_a\lambda}{\lambda_{za}}(\lambda_{za}^2-\lambda^2)^{-1/2} + 4\frac{|\Delta L_b|}{L_b}\frac{R_b\lambda}{\lambda_{zb}}(\lambda_{zb}^2-\lambda^2)^{-1/2} \qquad (3.42)$$

Table II lists the value of certain parameters for a simple accelerating field pattern produced by two templates. The required tolerances are also listed.

4. THE PRODUCTION OF TEMPLATES

The knowledge of both $\bar{E}$ and its derivative, or both $\bar{B}$ and its derivative on a closed surface suffices to determine the electromagnetic field inside that surface. Equivalently, the knowledge of the complex electric vector, $\bar{E}_c$, everywhere on the closed surface, suffices. In the following we will work with $\bar{E}_c$.

The situation is particularly simple if two of the complex components of $\bar{E}_c$ are always zero everywhere at the template surface. In this case it is

sufficient to illuminate the template with radiation polarized along one axis and modify the magnitude and phase of this $\bar{E}_c$ component only. Fortunately, this can be done in many cases, and in most of the following we will assume that it can be.

Even if $\bar{E}_c$ does not point along the same axis everywhere on the template, but the template can be divided into macroscopic regions over each of which $\bar{E}_c$ is polarized along a certain axis, different for different regions, then it is sufficient to illuminate each region with the appropriately polarized radiation, and otherwise the situation is the same as the one discussed in the previous paragraph. Finally, it may happen, that the desired field configuration is such that over certain regions of the surface of the chosen template, it is necessary to modify more than one component of $\bar{E}_c$. In this case, one has to use one of those materials, whose optical properties differ along two axes, and appropriately choose the angle of incidence. In this manner one can control the magnitude and phase of all $\bar{E}_c$ components independently, but that will not be discussed further.

Three methods of producing templates will be described.

A) *Explicit Calculation*

Once the field configuration along the trajectory has been decided, it is possible to use Maxwell's equations to continue the $\bar{E}$ and $\bar{B}$ fields to the surface of the template. Such a calculation was carried out in Sec. 3, where the field values at the surface of a cylindrical template were calculated and are given by Eqs. (3.8, 9, 10, 14, and 27). Actually, it is sufficient to calculate the fields at the template surface up to an arbitrary multiplicative constant, because, in any case, the field intensity at the trajectory will be proportional to the intensity of the radiation which passes through the template. For this reason, and although it could have been determined, the value of the constant Λ was not calculated in Eq. (3.27).

From the $\bar{E}$ and $\bar{B}$ one can calculate $\bar{E}_c$ over the inner (i.e., nearer to the trajectory) template surface. The template has to be so prepared, that when polarized radiation of wavelength λ enters through its outer surface, the $\bar{E}_c$ over the inner surface has the calculated magnitude and phase.

The magnitude of $\bar{E}_c$ can be controlled by choosing the transmissivity of the template as a function of position. That, in turn, can be achieved by increasing its reflectivity or absorbtivity where smaller transmitted intensity is desired. The phase of $\bar{E}_c$ can be controlled by choosing the optical thickness of the template as a function of position.

Reflectivity, absorbtivity, and optical thickness can all be varied by changing the geometrical thickness of the template ('etching') or by coating by reflective, absorbtive or optically active material. Etching and coating can be computer controlled. The template may be prepared on a blown up scale first, and subsequently reduced.

The resultant template, when illuminated by the appropriately polarized radiation, will produce fields with the correct magnitude, phase and polarization at the trajectory. In the terminology of Sec. 2, we say that this template is a phase controlled holograph.

The production of such phase controlled holographs is made simpler by the fact that the characteristic dimensions, D, of the pattern on the template surface are often large compared to λ, even if the characteristic dimensions, d, of the field pattern along the trajectory are comparable to λ. This can be expected whenever the (characteristic) distance of the template from the trajectory, R, is large compared to d:

$$D \gg \lambda, \text{ even if } d \approx \lambda, \text{ provided that } R \gg d. \tag{4.1}$$

Inequality (1) follows from the uncertainty principle: Let the trajectory be straight, and the template a plane parallel to the trajectory. Consider a characteristic bright area along the trajectory. Let $\bar{R}$ be a vector normal to the template, and going through the center of the bright area in question. If this bright area has dimension d along the trajectory, then the characteristic spread in the wave numbers parallel to the trajectory along the z axis is

$$\Delta k_z \approx \frac{1}{d} \tag{4.2}$$

resulting in an angular spread along $\bar{R}$ of

$$\Delta\Theta \approx \frac{\Delta k_z}{k_z} \approx \frac{\lambda}{d}, \tag{4.3}$$

which gives an illuminated area on the template surface, whose dimension parallel to the trajectory is

$$D \approx \Delta\Theta \cdot R = \lambda \frac{R}{d}, \tag{4.4}$$

in accordance with inequality (1). The well known diffraction pattern produced by a slit on a distant screen is an illustration.

B) *Measurement of $\bar{E}_c$ over the Template Surface*

a) The two-holograph method

A holograph[5] records on a screen the interference intensity pattern between two branches of a monochromatic light beam. One branch has relatively small intensity, and is modified by the object whose holograph one wishes to take, the other is intense, and is used for reference purposes. The intensity of the interference between two electric fields is proportional to

$$|E_{c1}+E_{c2}|^2 = |E_{c1}|^2 + 2|E_{c1}||E_{c2}|\cos\vartheta + |E_{c2}|^2, \tag{4.5}$$

where φ is the phase between E_{c1} and E_{c2}. If $|E_{c1}|^2 \gg |E_{c2}|^2$, then the last term can be neglected. The second term contains the information about the interference pattern. The information is ambiguous, because $\cos\varphi$ does not determine φ completely. With the exception of two special points, $\arccos\varphi$ is double valued. The holograph can not distinguish between the two sets of φ, and if one attempts to reconstruct the image of the original object from the holograph, *two* images are produced. One is the correct image, and the other, the so-called 'twin image', is spurious. The two images lie at equal distances from, but on opposite sides of the holograph.

It will now be shown that one can use interference patterns to determine completely, but one has to prepare *two* suitable holographs of the same object instead of only one. The first holograph is taken in the usual manner, and records the usual information given in Eq. (5). The second holograph is taken on the same screen, and with the same object, but with the phase of the reference beam shifted by $\pi/4$. The shift can be achieved, for example, by introducing a transparent plate of the appropriate optical thickness into the path of the reference beam. The second holograph will then record at every point of the screen the quantity

$$|iE_{c1}+E_{c2}|^2 = |E_{c1}|^2 + 2|E_{c1}||E_{c2}| \times \cos\left(\vartheta+\frac{\pi}{4}\right) + |E_{c2}|^2, \tag{4.6}$$

where the last term can again be neglected whenever $|E_{c1}|^2 \gg |E_{c2}|^2$. The information about the interference pattern is contained in the second term. Together with the second term in Eq. (5), it completely determines both $|E_{c2}|$ and φ, which is equivalent to determining E_{c2} completely. Clearly, the same method is applicable, if the shift in phase in the reference beam of the second holograph is not exactly $\pi/4$. However, a shift $\pi/4$ or $3\pi/4$ will permit the smallest errors in determining φ.

To produce a phase controlled holograph to be used as a template, one can proceed as follows. Take two ordinary holographs on the template surface as just described. Use as the second branch of the radiation, light from an object placed along the particle trajectory (for example, a grating with openings d_b wide and d_d apart) which has the property that it produces the desired field configuration along the trajectory. The two holographs then contain all information about E_c on the template surface, and so E_c need not be calculated explicitly. This information can then be used to produce the template in the same manner as described in (A).

It is, of course, possible to make certain straightforward changes in the geometry for purposes of taking holographs. Instead of using as an object a string of light and dark areas along the trajectory, and taking its holograph on the surface of a cylinder, one can 'cut the cylinder and roll it open' to form a plane, and then take the holograph of an ordinary line grating on this plane. The templates produced from these holographs can subsequently be rolled up, and will produce the desired field configuration of light and dark areas along their axes.

b) Measurement on models

Instead of working with short wavelengths, one can produce large scale models and scale up the

wavelength of the radiation correspondingly. The procedure is then the same as in (a), except that one can determine the E_c in several different ways, including the use of macroscopic measuring objects and this may be preferred in certain cases over the method of taking holographs.

C) *A Holograph Serving as Template*

In many cases a simple holograph can serve as template. This happens whenever the effect of the twin image does not seriously interfere with the acceleration of particles. There are two reasons why the effect of the twin image can often be neglected.

First, the twin image is produced on the far side (away from the trajectory) of the holograph. The radiation associated with it near the trajectory appears to come from far away (see Fig. 4) and may,

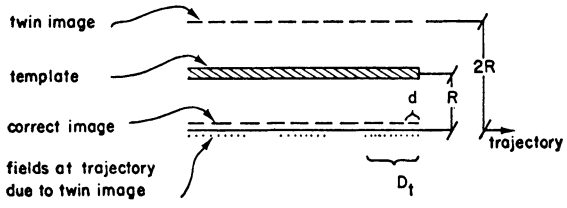

FIG. 4. If the template is an ordinary holograph, then radiation passing through it produces two images. One is the correct image and is real, the other is the twin image, and is virtual. The field configuration due to the correct image has characteristic dimensions d along the trajectory, while that due to the twin image has D_t.

therefore, have lower intensity along the trajectory than the radiation associated with the correct image. However, the geometry can be such that the two intensities are about equal. Such is the case if the template is a cylinder whose axis is the trajectory along the z axis, as would be obtained by rotating Fig. 4 around the trajectory by 360°.

Second, even if the two average intensities are about equal along the trajectory, the acceleration of the particles due to the twin image is often negligible. (See Fig. 4.) This is a consequence of Eq. (4): The characteristic dimension parallel to z of the field configuration in the twin image is d, just as for the correct image. The field pattern along the axis due to this image has, according to Eq. (4), characteristic dimensions D_t parallel to z, where

$$D_t \approx \lambda \frac{2R}{d}. \tag{4.7}$$

If the two patterns have the same average intensity along the trajectory, and if d and D_1 are both $\gtrsim \lambda/2$, then the maximum kinetic energy gained by the particle in one connected bright area is independent of the size of that area as explained in Sec. 1. Therefore, the twin image, with its larger patterns, is less efficient in accelerating particles than the correct image. The ratio of efficiencies is

$$\frac{\Delta K_t}{\Delta K} \approx \frac{d}{D_t} \approx \frac{d^2}{2R\lambda}, \tag{4.8}$$

which is, for $d \approx \lambda$, about $\lambda/2R$, often a very small number. Therefore, the undesired acceleration experienced by the particle due to the existence of the twin images is often negligible. This result also follows from the discussion in the paragraph after Eq. (A1.4d). Expand the field configuration along the trajectory into Fourier components, and recall that the maximum energy which a component can transfer to the particle is proportional to

$$\Omega_z^{-1} = \left(\frac{2\pi}{\lambda_z} - \frac{2\pi}{Tv_0}\right)^{-1}.$$

In an efficient configuration, components with small Ω_z dominate. In the twin image the sign of λ_z is opposite to what it is in the correct image, so that small Ω_z in the latter corresponds to

$$\left(-\frac{2\pi}{\lambda_z} - \frac{2\pi}{Tv_0}\right)$$

in the former. The accelerating efficiency of the twin image relative to that of the correct image is of the order of

$$\left(\frac{1}{\lambda_z} - \frac{1}{Tv_0}\right) \Big/ \left(-\frac{1}{\lambda_z} - \frac{1}{Tv_0}\right),$$

which for $L \gg \lambda$, and $\Omega_z \lesssim 1$ is of the order of $\lambda/2L$.

As an example, assume that we want to make an infinitely long cylindrical template which will produce a Fourier component with wave number k_z along the axis.

Equation (3.14b) shows that for any finite $\lambda_z \geqq \lambda$ one can choose R such that at $r = R_c$ the radial component of the electric field $E_r(t, z, r = R_c) = 0$ for all z and t (except during turning on (and off) of the radiation).

Let the template consist of a reflecting coating on an optically inactive cylinder, and vary the surface reflectivity (or transmissivity) of the template as a function of z. Let the thickness of the coating be $\ll \lambda$, and the radius of the template $R = R_c \gg \lambda$. Let L satisfy Eq. (3.29), and choose

$$c'_{k_z} = \begin{cases} 1/2, \text{ if } |k_z'| = |k_z| \\ c_0, \text{ if } k_z' = 0 \\ 0 \text{ otherwise} \end{cases} \tag{4.9}$$

where k_z is such that

$$2L\left(\frac{1}{\lambda_z} - \frac{1}{Tv_0}\right) = \frac{1}{2},$$

and c_0 is an arbitrary constant. The electric field on the surface of the coating is then, according to Eq. (3.14):

$$E_z(t, z, r = R_c) \approx \mathrm{Re}\left\{ i\frac{\omega}{c} e^{-i\omega t}\left[c_0 + (\cos k_z z)\left(\frac{2}{\pi\kappa_z R_c}\right)^{1/2} \cos\left(\kappa_z R_c - \frac{\pi}{4}\right)\right]\right\}, \tag{4.10a}$$

$$E_r(t, z, r = R_c) \approx 0$$

As c_0 approaches $(2/\pi\kappa_z R_c)^{1/2} \cos(\kappa_z R_c - \pi/4)$, the z dependence of E_z at $r = R_c$ approaches $(1 + \cos k_z z)$. In this limit, when the template is illuminated by a convergent cylindrical wave polarized parallel to the z axis, the electric field produced along the axis will be (neglecting multiple reflections)

$$E_z(t, z, r = 0) \approx \mathrm{Re}\left\{ i\frac{\omega}{c} e^{-i\omega t}\left[\left(\frac{2\pi}{\lambda\kappa_z}\right)^{1/2} \frac{\cos(\kappa_z R_c - \pi/4)}{\cos(2\pi R_c/\lambda - \pi/4)} + \cos k_z z\right]\right\}, \tag{4.10b}$$

$$E_r(t, z, r = 0) \approx 0 .$$

The Fourier components with $k_z' = k_z$, $-k_z$, and 0, give the correct image, the twin image and the background term respectively. Acceleration is done mainly by the correct image, the other two terms contribute to the acceleration (or deceleration) of the particle only negligibly when $L \gg \lambda$, in agreement with what was said above. The configuration given by Eq. (10) is just a sequence of light and dark areas super-imposed on a background of intermediate brightness, it is a configuration of the type discussed in Sec. 2.

Once the optical properties on the template surface are given, the approximate form of the field produced by it is often easy to see. However, finding the exact solution satisfying all the boundary conditions, may be difficult. One particular template for which the solution can be calculated exactly, is an infinite plane strip grating consisting of infinitely long parallel strips of a perfectly conducting material of width d and separated from each other by a distance d. Although this template is not cylindrical, 'rolling it up' as described in subsection *B.a.* would lead to a cylindrical template of the type discussed in Sec. 3. The field produced by such a plane template is given in Appendix 2.

Whereas the twin image and the background term often (particularly at lower energies) do not do much harm, their existence is wasteful. For this reason, it is desirable to eliminate them.

If the template is an ordinary holograph, then its reproduction is particularly simple: new templates can be obtained by simply photographing the original one.

5. SYNCHRONIZERS

After a particle leaves an accelerating unit and before entering the next one, it passes through a synchronizer. The purpose of the synchronizer is to insure that the particle will be further accelerated by each successive accelerating unit.

In most cases of interest to us, the characteristic

dimensions of the accelerating field configuration along the trajectory are of the order of λ, the wavelength of the radiation, and the particle travels with a velocity $v \approx c$. The time the particle spends in one accelerating bucket, is of the order of

$$\frac{\lambda}{8v} \approx \frac{\lambda}{8c} = \frac{\pi}{4\omega}.$$

When $\omega \lesssim 10^{11}$, then these times are long, and synchronization of the two successive accelerating units present no insurmountable problem. On the other hand, if $\omega > 10^{11}$, the characteristic times τ in question are shorter than, or equal to 10^{-10} seconds, beyond the limit of feasibility. Nevertheless, the necessary synchronization can be achieved, as will be outlined in the present section. The discussion will be restricted to the frequency range in, or near, the visible—a range of particular interest to us.

Let us remark that the most straightforward way to synchronize two successive accelerating units would be to synchronize the two successive lasers which belong to them, using a standard reference beam travelling parallel to the trajectory. Unfortunately, present amplification techniques are not up to this task, and one has to proceed differently.

In the method to be described here, synchronization is achieved in two steps:

1) The lasers are synchronized with the accuracy of $\tau_M \approx 10^{-9}$ or 10^{-10} seconds.

2) More accurate synchronization is achieved by appropriately shaping the particle orbits.

1) The lasers are fired within the presently feasible accuracy of $\tau_M \approx 10^{-9}$ or 10^{-10} seconds, which insures that radiation will be present in the accelerating unit whenever the particles pass through it. This can always be done by simply making the laser pulse longer than ideal by the amount τ_M. Then some radiation will reach the trajectory either before or after the particles pass there, and will be wasted, but all particles within the accelerating unit will always be in the presence of radiation fields. These fields may either accelerate, or decelerate the particles.

2) In order that the average field be always accelerating, an accelerating bucket has to wait for the particle as it enters each accelerating unit. The bucket lasts only of the order of 10^{-15} seconds in the visible range. Since the fields can not be timed with such accuracy, we intend to time the particles by appropriately modifying their trajectory.

Consider two successive accelerating units, A_1 and A_2. The lasers belonging to them are S_1 and S_2 respectively. (See Fig. 5.) The radiation from

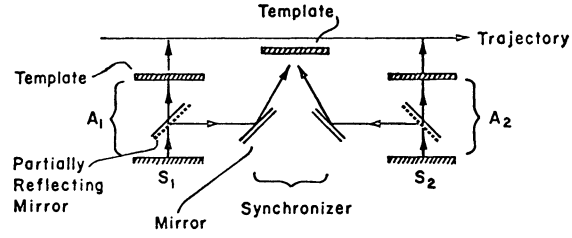

FIG. 5. Two successive accelerating elements are A_1 and A_2, the lasers belonging to them are S_1 and S_2. Radiation from S_1 is split by a partially reflecting mirror into R_{1A} and R_{1S}. The R_{1A} irradiates the template belonging to A_1, while R_{1S} irradiates the template belonging to the synchronizer. The R_{2A} and R_{2S} are defined similarly.

S_1 is R_1, and is split by a partially reflecting mirror into R_{1A} and R_{1S}. The R_{1A} irradiates the template belonging to A_1, while R_{1S} irradiates the template belonging to the synchronizer. The R_1, R_{2A}, and R_{2S} are defined similarly.

The synchronizer consists of a template irradiated by both R_{1S}, and R_{2S}.

We say that a laser is in phase with the particle, if the particle experiences maximum acceleration in the accelerating unit to which the laser belongs. Suppose that a laser is not in phase with the particle, but that if its phase were shifted by $-\varphi$, then it would be. Then we say that the laser is out of phase with respect to the particle by φ.

Choose the optical pathlengths L_1 (between A_1 and the synchronizer), and the similarly defined L_2 in such a manner, that if both S_1 and S_2 are in phase with the particle, then

$$L_2 - L_1 = \frac{\lambda}{2} + \text{integer} \cdot \lambda. \tag{5.1}$$

Let the intensity of R_{1S} be equal to that of R_{2S}. Then whenever both S_1 and S_2 are in phase with the particle, the electromagnetic fields due to R_1 and R_2 cancel at the synchronizer, and the net field

there will be close to zero. On the other hand, if S_1 is in the phase with the particle, but S_2 is out of phase with respect to it by $\varphi = \pi$, then R_1 and R_2 will be in phase at the synchronizer, and a large electromagnetic field is produced there.

a) Let the synchronizer have cylindrical symmetry around the straight trajectory which is chosen to be the z axis. The template is arranged to produce fields which have the general features shown in Fig. 2. Assume that S_1 is in phase with the particle, and $v \approx c$. In general, while passing through the synchronizer, the particle will experience a force F_b in each bright area, which is proportional to

$$\int_0^{\pi} d\alpha[\sin\alpha + \sin(\alpha + {}_{\varphi} + \pi)] = 2[1 + \cos(\varphi + \pi)]$$

After passing through the whole synchronizer, the net force exerted by the fields in the synchronizer on the particle will be proportional to the product of F_b with the number of bright areas per unit length n, and the length of the synchronizer L_S

$$F_s = F_0\, 2L_s n[1 + \cos(\varphi + \pi)]. \qquad (5.2)$$

The F_0 is a constant of proportionality, and depends on the intensity of the radiation R_{1S} (or R_{2S}). The intensity of R_{1S}, the n, and L_S can be so chosen, that as a result of passing through the synchronizer, the particle will be accelerated so that its time of flight through the synchronizer will be decreased by just $\Delta t = \lambda/2v$ when $\varphi = \pi$. (See Fig 6a.) Then, if S_2 were out of phase by π relative to the particle as it leaves A_1, the synchronizer would accelerate the particle just so that it will be in phase with S_2 as it arrives at A_2.

Actually, when $\cos(\varphi + \pi) \neq \pm 1$, then φ can not be determined uniquely (up to $n' \cdot 2\pi$), but a double valued ambiguity arises. This can be resolved by simply adding a second section to the synchronizer in which d_b has a different value, or in which $L_1 - L_2$ is changed. For example, choosing $L_2 - L_1 = \lambda/4 + (\text{integer} \cdot \lambda)$ and leaving d_b unchanged will lead to a net force F which will be a function of $\sin(\varphi + \pi)$ instead of $\cos(\varphi + \pi)$, and φ can then be determined uniquely.

The method just described is of only limited usefulness. The F_0 and L_S are limited by the power output of S_1 or S_2 and by the coherence length of the radiation. The n is limited by the length L_S. On the other hand as γ increases, the force needed to accelerate or decelerate the particle increases. Assuming that S_1 and S_2 are each capable of a power output of 10^{14} Watts in short pulses, and coherence can be maintained in the synchronizer over a trajectory length of $2 \cdot 10^2$ cm, one finds that depending on the geometry and other details

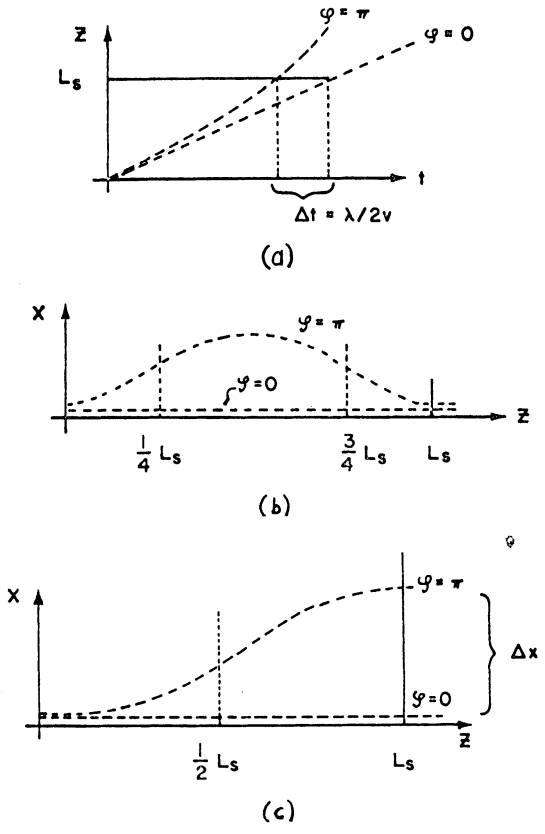

FIG. 6. (*a*) The figure shows the particle trajectories in the synchronizer located between two accelerating units: A_1 and A_2. Without the synchronizer, the laser belonging to A_2 would be out of phase with the particle by the phase angle φ. The trajectory depends on φ: the particle is accelerated in the synchronizer along a straight trajectory when $\varphi \neq \pi$, but not otherwise. When $\varphi = \pi$, then the particle is so accelerated that it leaves the synchronizer at a time Δt earlier than the unaccelerated particle would. (*b*) The particle makes a detour in the synchronizer. Its pathlength depends on φ: it is the shortest for $\varphi = 0$. The speed of the particle is unchanged to first order. (*c*) The particle leaves the synchronizer with an x coordinate which depends on φ. When $\varphi = 0$, then x at exit is zero. When $\varphi = 0$, then $x = \Delta x$. The speed of the particle, as well as its pathlength inside the synchronizer, are unchanged to first order.

of the accelerator, the synchronizer just described can be used as $\lambda_r \to \lambda$, for protons with energy

$$\mathscr{E}_p \lesssim 10^2 \text{ GeV}, \tag{5.3a}$$

and for electrons with energy

$$\mathscr{E}_e \lesssim 10^3 \text{ GeV}. \tag{5.3b}$$

b) Denote one oft he Cartesian axes perpendicular to z by x. Let the synchronizer be reflection symmetric across the (x, z) plane. The d_b are chosen as in (a), but the template and the radiation polarization is so prepared, that the electric field polarization at the z axis is along $\hat{x}$. The net force is still given by Eq. (2), but it points along $\hat{x}$. The particle is accelerated along $\hat{x}$. (See Fig. 6b.) The template is such that in the first quarter of the synchronizer, F_S is parallel to x, in the second and third quarters it is anti-parallel, and in the fourth quarter, it is parallel again. As a result of these forces acting on it, the particle describes a detour inside the synchronizer, but returns to the z axis at L_S, and as it leaves the synchronizer, its velocity is again parallel to z. The length of the trajectory along the detour is Δl longer than it would have been had the particle travelled along the z axis. The particle takes $\Delta t = \Delta l/v$ time longer to travel across the synchronizer than it would have taken, had it travelled straight along the z axis. The F_0, n, L_S can be so arranged that $\Delta t = \lambda/2v$ when $\varphi = \pi/2$. Again, an ambiguity in φ results, but can be resolved as explained under (a) above.

The efficiency of the synchronizer is again limited by the power output of S_2 and S_1 and the coherence length of the radiation. We calculate the path difference between the two trajectories shown in Fig. (7b), assume that $v \approx c$ everywhere in the synchronizer, and find that depending on the details of the geometry and design, $\Delta l \approx 10^{-2} \left| qE_{x\|\text{av}} \right|^2 L_S{}^3/\mathscr{E}^2$. Therefore, this synchronizer can induce a time interval $\Delta t = \lambda/2v$ as long as the total energy $\mathscr{E}$ of the particle with charge q satisfies

$$\mathscr{E} \lesssim \frac{1}{7} q \left| E_{x\,\text{av}} \right| l \sqrt{\frac{l}{\lambda}}, \tag{5.4}$$

where E_{av} is the average (in the sense of Eq. (2.3)) of the absolute value of the electric field along the x axis. Assuming again a laser power of 10^{14} Watts, that coherence can be maintained in the synchronizer over a trajectory length of $2 \cdot 10^2$ cm, and also assuming $\lambda = 10^{-4}$ cm, $l = 10$ cm, we obtain $\mathscr{E} \lesssim 10^3$ GeV, as $\lambda_r \to \lambda$.

The restmass of the particle does not enter into Eq.(4); it is the same for electrons and protons. The reason is that in contrast to (a), in this synchronizer the velocity of a particle (and therefore its γ), changes only in second order. The time difference is due to a change in pathlength, not due to a change in speed.

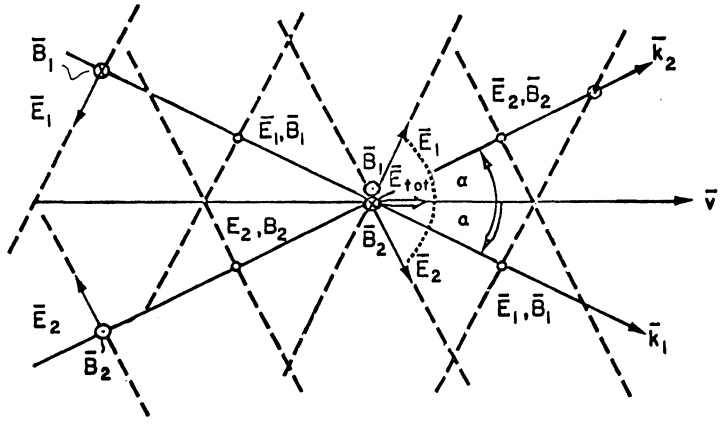

FIG. 7. Two monochromatic plane polarized electromagnetic plane waves are incident on a positively charged particle travelling with velocity $\bar{v}$. The momenta of the two waves, $\bar{k}$, $\bar{k}_2$, and the electric field vectors $\bar{E}_1$, $\bar{E}_2$, as well as $\bar{v}$ are all coplanar. The angles $(\bar{k}_1, \bar{v})$ and $(\bar{v}, \bar{k}_2)$ are equal and are denoted by α. The phases of the waves are so chosen that the total magnetic field and the total transverse (to $\bar{v}$) component of the electric field at the trajectory are zero. The dashed lines represent planes of constant phase in the two waves. The values of the electric and magnetic fields in these planes are shown, $\otimes$ and $\odot$ mean into and out of the plane of the figure. The resultant field at the particle trajectory is parallel to $\bar{v}$, and accelerates the particle.

(c) Choose the coordinate axes as in (b) and let the synchronizer again be reflection symmetric across the (x, z) plane. As in (b), the force acting on the particle is along the x direction, and its magnitude is described by Eq. (2). The difference between the case discussed under (b), and the synchronizer to be discussed here is that in this case, the forces acting on the particle switch sign only once. In the first half of the synchronizer they are parallel to x; in the second half, they are antiparallel to x. (See Fig. 6c.) As a result, when the particle leaves the synchronizer, it will always have a velocity parallel to the z axis, but its x coordinate Δx at that point may be nonzero. The template belonging to A_2 is prepared in such a manner, that the accelerating field configuration in A_2 is not cylindrically symmetric, but, near the x axis, it is reflection symmetric along a narrow strip in the (x, z) plane. In this strip, the accelerating buckets are shaped so that surfaces of constant field intensity at any moment are perpendicular to the (x, z) plane, and their intersection with that plane is proportional to arc cos z.

When $\varphi = 0$, the net electromagnetic field in the synchronizer is zero, and the particle travels along the z axis. When $\varphi = \pi$, the particle is deflected along x, but its velocity $\bar{v}$ is not changed in the first approximation, because the force is very close to being perpendicular to v everywhere in the synchronizer. Furthermore, the time of flight of the particle does not change either in the first approximation, as long as $\Delta x \ll L$. In the following, we assume that this is so. As the particle enters A_2, it will experience the eccelerating bucket at a point Δx from the x axis. At this point, the position of the bucket is just such that the bucket there is in phase with the particle. The Δx need be only large enough to permit the necessary variation of the accelerating field in A_2 within Δx. When the φ is between 0 and π, the particle will arrive at A_2 with an x coordinate between 0 and Δx. The ambiguity in φ can be resolved as before, and the particle will be in phase with the accelerating bucket at that particular x value.

The very small displacement of the trajectory along x which will leave its length unchanged in the first approximation will be enough to achieve synchronization with A_2. We calculate $|\Delta_x|$ in terms of the particle energy $\mathscr{E}$ and $|F_\perp|$, then express $F_\perp$ as $qE_{x\|\mathrm{av}}$, and obtain $|\Delta_x| = |qE_{x\|\mathrm{av}} \times L_S^2/4\mathscr{E}|$. The exact coefficient of proportionality depends on the details of the design. The $|E_{x\|\mathrm{av}}|$, and L_S are limited from above by the power and coherence length of the radiation; $|\Delta x|$ is limited from below by λ, therefore, assuming $\Delta x \approx 5\lambda$,

$$\mathscr{E} \lesssim 5 \cdot 10^{-2} |qE_{x\|\mathrm{av}}| L_S^2/\lambda. \tag{5.5}$$

For the values of parameters assumed in (b), but choosing $L_S = 20$ cm, we find $\mathscr{E} \lesssim 10^6$ GeV.

ACKNOWLEDGEMENTS

I wish to to thank H. W. Lefevre, M. D. Girardeau, G. D. Mahan, J. W. McClure, M. J. Moravcsik, K. J. Park, and G. H. Wannier for some very interesting conversations concerning this subject. I am particularly grateful to A. M. Sessler for his valuable comments.

APPENDIX 1

To better understand Eqs. (3.25), (3.27), (3.28) and (3.29), let us consider two monochromatic plane polarized electromagnetic plane waves with equal amplitudes and circular frequency ω, incident on a particle with charge q travelling in vacuum as shown in Fig. 7. The phase velocity of light in vacuum is c_φ. The amplitude of the electric field in either wave is E_0. The electric field (as seen from the laboratory) at the position of the particle points along $\bar{v}$, and at the time t its value is

$$\bar{E} = E_{||}\hat{z} = 2E_0(\sin\alpha)\sin\left[\omega\left(1 - \frac{v}{c_\varphi}\cos\alpha\right)t\right]. \tag{A1.1}$$

The increase in the kinetic energy, K, of the particle can be calculated if $v(t)$ is known. Assuming that $v(t)$ is a constant during the process (a good approximation if $v \approx c$),

$$\Delta K(t) = K(t) - K(0) = q2v_0 E_0 \times (\sin\alpha)\frac{1-\cos\Omega t}{\Omega}, \tag{A1.2}$$

where

$$\Omega \equiv \omega\left(1 - \frac{v}{c_\varphi}\cos\alpha\right). \tag{A1.3}$$

The $\Delta K(t)$ reaches its locally (in t) maximum values

$$\Delta K_{\max}(t) = \frac{4LqE_0 \sin\alpha}{\Omega t} = \frac{4L_m qE_0 \sin\alpha}{\pi + m2\pi} \qquad \text{(A1.4a)}$$

at times

$$t_m = \frac{1}{\Omega}(\pi + m2\pi) \qquad \text{(A1.4b)}$$

where

$$L \equiv v_0 t \ , \qquad L_m \equiv v_0 t_m, \qquad \text{(A1.4c)}$$

and m is any integer. The time average of ΔK is zero.

If $|\Omega|$ can be made small enough, then $\Delta K_{\max}$ can be made arbitrarily large. Since $\cos\alpha \leqq 1$, the Ω can be zero only if $v < c$. Because of $\boldsymbol{v} < c$, one has to have $c_\varphi < c$ for this to happen. The latter condition can be satisfied only by electromagnetic fields which decay exponentially as a function of the distance from their source. Such fields can be used to accelerate particles, as described in Refs. 1 and 7. However, because of their exponentially decaying nature, these fields tend to reach their highest value at their source. Much higher fields can be achieved when $c_\varphi \geqq c$ and in the following we will consider the latter case.

If $|\Omega|$ can not be made arbitrarily small, then $\Delta K_{\max}$ is limited from above. If the particle is injected into the field at time zero, and removed from it at a later time t_m, then it can acquire $\Delta K_{\max}(t_m)$ energy. According to Eq. (4), this energy is larger if L_m is larger, and for any L_m if Ω is smaller i.e., if the field experienced by the particle changes more slowly so that the particle 'stays in phase with the field' for a longer time.

Returning to Eq. (3.25), let us introduce the notation

$$\Omega_z \equiv 2\pi\left(\frac{1}{\lambda_z} - \frac{\omega}{2\pi v_0}\right), \qquad \lambda_z \equiv 2\pi/k_z, \qquad \text{(A1.4d)}$$

and consider the case when c_{k_z} is zero for all, except one particular k_z. The right hand side is then

$$\mathrm{Re}\left\{c_{k_z} 2iq\frac{\omega}{c}L\frac{\sin\Omega_z L}{\Omega_z L}\right\}.$$

The absolute value of this expression is maximum in a neighborhood of any $L > Tv_0$, if $\Omega_z L = (\frac{1}{2}+m')\pi$, where m' is any integer. This happens if Eq. (3.29) is satisfied, since $2L/\lambda_z$ has to be an integer. The local maximum for any L is largest if Ω_z is smallest, i.e., if $\Omega_z = \pi/2$. This shows that those waves accelerate the particle most efficiently, for which Ω_z is smallest, as one would expect from the simpler case described by Eq. (4). According to Eq. (3.27), the coefficients c_{k_z} multiplying the Fourier component with k_z is proportional to Ω_z^{-1}, so that the wave which accelerates most efficiently occurs with the largest amplitude. However, the coefficients multiplying the other Fourier components are given to be nonzero by Eq. (3.27). To understand the reason for this, recall that the field energy stored in a Fourier component is proportional to $|c_{k_z}|^2$, so that it is more efficient to distribute the available field energy over several Fourier components, rather than concentrate it all into one. For a given ε, the highest acceleration results if approximately $c_{k_z} = \mathrm{const}/\Omega_z$. More exactly, the best choice is $c_{k_z} = \mathrm{const}\,\Omega^{-1}[1-(\lambda/\lambda_z)^2]^{3/2}$, according to Eq. (3.27). The factor $[1-(\lambda/\lambda_z)^2]^{3/2}$ biases the field configuration in favor of larger λ_z, and is due to the fact that for the same value of $|c_{k_z}|^2$, waves with larger λ_z require less energy, as is shown by the presence κ_z^{-3} in Eq. (3.19).

APPENDIX 2

Consider an infinite plane consisting of a sequence of infinitely long perfectly conducting strips of width d, separated from each other by a distance d. The plane is located in vacuum. It is perpendicular to the z axis. The strips are parallel to the x axis, and $\hat{y} \equiv \hat{z} \times \hat{x}$. The origin of the coordinate frame is located on the plane, at the edge of one conducting strip, so that this strip crosses the positive (as opposed to the negative) y axis. This determines the location of the origin up to arbitrary displacements along x, and displacements by integer multiples of d along y (both types of displacements are physically irrelevant). A monochromatic electromagnetic plane wave of the form $e^{-i(\omega t+kz)}$ approaches the plane along the positive z axis. The wave is plane polarized, with the electric vector parallel to $\hat{x}$. (When the magnetic

field is parallel to $\hat{x}$, then the solution can be obtained from the present case by applying Babinet's principle).

The resulting electric field will be polarized along $\hat{x}$, will be independent of x, and will have the form $e^{-i\omega t}E_x(y,z)$. The $E_x(y,z)$ was given by L. A. Weinstein[8].

$$E_x = e^{-ikz} + \sum_{n=-\infty}^{+\infty} A_n e^{ik(y\sin\varphi_n + z\cos\varphi_n)}; \text{ for } z > 0, \tag{A2.1}$$

$$E_x = \sum_{n=-\infty}^{+\infty} B_n e^{ik(y\sin\varphi_n - z\cos\varphi_n)}; \text{ for } z < 0,$$

where

$$A_0 = \tfrac{1}{2}(-1+R_0), \quad B_0 = \tfrac{1}{2}(1+R_0) \tag{A2.2a}$$

$$A_n = B_n = \tfrac{1}{2}R_n, \text{ for } n = \pm 1, \pm 2, \ldots. \tag{A2.2b}$$

$$\sin\varphi_n = \frac{\lambda}{2d}n, \quad \cos\varphi_n = \left[1-\left(\frac{\lambda n}{2d}\right)^2\right]^{1/2}, \quad n = \pm 1, \pm 2, \ldots. \tag{A2.3}$$

The coefficients R_n are

$$R_{2s} = \frac{-i}{w_{2s}d}\left(\frac{2k}{k+w_{2s}}\right)^{1/2}\frac{\varphi_+(k)\varphi_+(w_{2s})}{\psi_+(k)\psi_+(w_{2s})}, \tag{A2.4a}$$

$$R_{2s+1} = \frac{i}{w_{2s+1}d}\left(\frac{2k}{k-w_{2s+1}}\right)^{1/2}\frac{\psi_+(w_{2s+1})\varphi_+(k)}{\varphi_+(w_{2s+1})\psi_+(k)}, \tag{A2.4b}$$

$$R_{-n} = (-1)^n R_n, \tag{A2.4c}$$

$$s = 0, 1, 2, \ldots, \quad n = 0, 1, 2, \ldots,$$

where

$$\psi_+ = \left(2\cos\frac{kd}{2}\right)^{1/2} e^{i(kd/2\pi)M_+(\tau)} \prod_{n=1}^{\infty}\left(1+\frac{w}{w_n}\right)e^{(\tau_n-\tau_{n-1})(dw/2\pi)}, \tag{A2.5a}$$

$$\varphi_+ = \left[-2i\left(\sin\frac{kd}{2}\right)\left(1+\frac{w}{k}\right)\right]^{1/2} e^{i(kd/2\pi)M_+(\tau)} \prod_{n=1}^{\infty}\left(1+\frac{w}{w_n}\right)e^{(\tau_n-\tau_{n-1})(dw/2\pi)}, \tag{A2.5b}$$

and the remaining symbols appearing in Eqs. (4) and (5) are defined in terms of d, k, w and w_n, as follows. The τ and $M_+(\tau)$ are defined by the equations

$$\sin\tau = \frac{w}{k}, \quad \cos\tau = \left[1-\left(\frac{w}{k}\right)^2\right]^{1/2}, \tag{A2.6}$$

and

$$M_+(\tau) = \left(\frac{\pi}{2}-\tau\right)\left[1-\left(\frac{w}{k}\right)^2\right]^{1/2} + \frac{w}{k}. \tag{A2.7}$$

The definition of w_n depends on whether w_n appears in the argument of a ψ_+ or a φ_+ function. When w_n appears in the argument of a ψ_+ function, then w_n are zeros of the function $[1+\exp(id\sqrt{k^2-w^2})]$, i.e.

$$w_n = \left\{k^2 - \left[\frac{2\pi}{d}(n+\tfrac{1}{2})\right]^2\right\}^{1/2}.$$

When w_n appears in the argument of a φ_+ function, then w_n are the zeros of the function $[1-\exp(id\sqrt{k^2-w^2})]$, i.e.

$$w_n = \left\{k^2 - \left(\frac{2\pi}{d}n\right)^2\right\}^{1/2}.$$

(The $\mathrm{Im}(w_n)$ is always defined to be $\geqq 0$.)

REFERENCES

1. Paul L. Csonka, 'Particle Acceleration by Intense Coherent Electromagnetic Waves', University of Oregon Preprint, May 25, 1972, N. T. 049/72.
2. E. M. McMillan, *Phys. Rev.*, **79**, 498 (1950).
3. A. A. Kolomenskii and A. N. Lebedev, *Dokl AN SSSR*, **145**, 1259 (1962); *Zh. eksperim. i teor. fiz.*, **44**, 261 (1963) (*Soviet Physics Doklady*, **7**, 745 (1963), *Soviet Physics JETP*, **17** 179 (1963).
4. R. B. Palmer, Brookhaven National Laboratory preprint, BNL 16440.
5. D. Gabor, *Nature*, **161** 777 (1948), *Proc. Roy. Soc. (London)*, **A197**, 454 (1949).
6. The subscript 'Av' is to be distinguished from the subscript 'av'. The latter means averaging over times Δt as discussed earlier.
7. S. A. Kheifets; *Proc. 8th Conf. High Energy Accelerators, CERN*, 1971, p. 597.
8. Lev Albertovich Weinstein, *The Theory of Diffraction and the Factorization Method* (Generalized Wiener-Hopf Technique) (The Golem Press, Boulder, Colorado, 1969). I am grateful to A. M. Sessler for pointing out to me the existence of this work.

Received 13 February 1973;
and in final form 16 April 1973